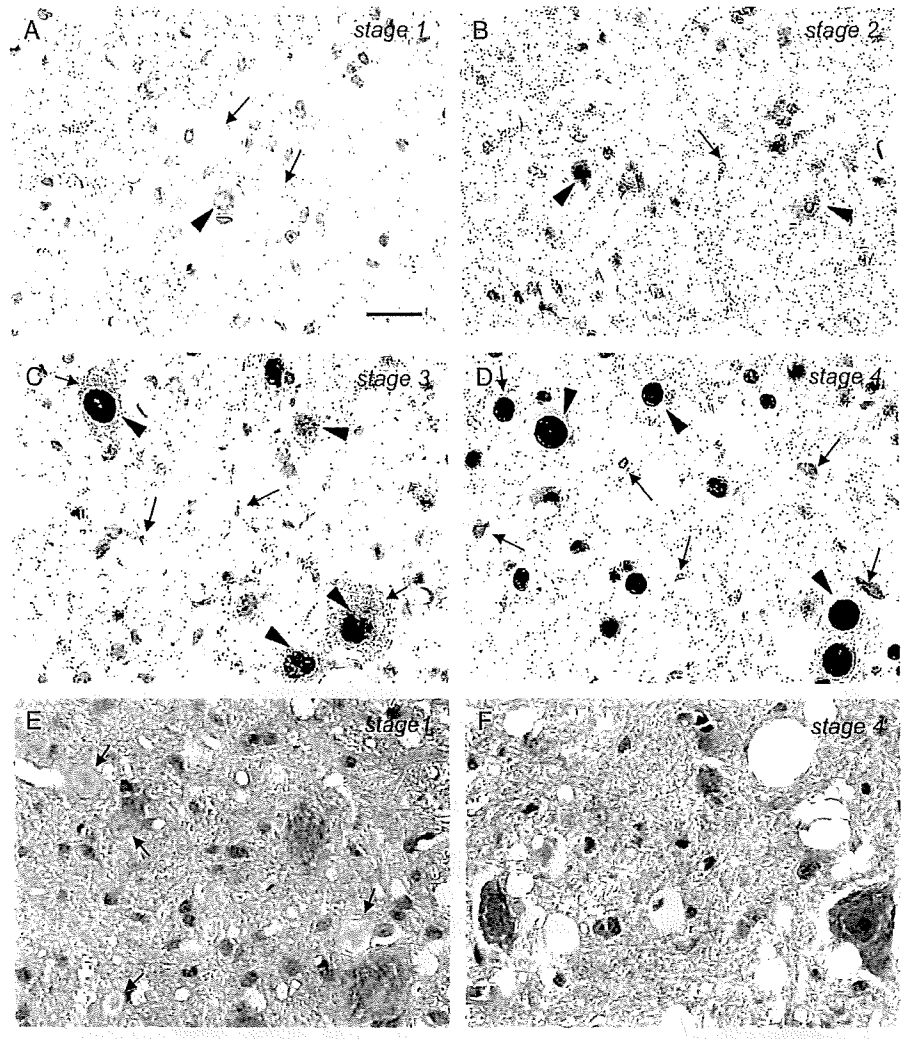

FIGURE 5. Four stages of TAR DNA binding protein (TDP) immunoreactivity in spinal cord neuron nuclei of G1L mice. **(A)** In Stage 1, nuclear immunoreactivity (arrowhead) is weak. Lewy body-like hyaline inclusions (LBHIs) (arrows) are only faintly stained or negative. **(B)** In Stage 2, nuclear immunoreactivity of neuron nuclei (arrowheads) is similar to that of normal littermates (Fig. 4A). Neurites or tiny vacuoles (arrow) also show immunoreactivity. **(C)** Immunoreactivity in Stage 3 in most of the nuclei (arrowheads) is stronger than in the normal control, but less than in Stage 4. There is diffuse and punctate cytoplasm staining and immunoreactivity in neurites (arrows). **(D)** Nuclear immunoreactivity in Stage 4 is very strong (arrowheads), and there are numerous TDP-positive neurites (arrows). **(E)** Prominent LBHIs (arrows) are evident in a Stage 1 mouse. **(F)** In a Stage 4 mouse, there are many vacuoles detected, but there is no LBHI formation. Immunohistochemistry for TDP (**A–D**); hematoxylin and eosin stain (**E, F**). Scale bar = 50 μm.

slow course than in those with a rapid course (Wilcoxon rank sum test: neuronal inclusions, p = 0.0002; glial inclusions, p = 0.0002). The numbers of large neurons (>37 μm) were also lower in SALS patients with a slow course than in those with a rapid course, although the level of significance (p = 0.0264) was lower than that for TDP-positive inclusions. The relationships among the numbers of large neurons, and TDP-positive inclusions in neurons and glia were not significant in SALS patients as a whole (Spearman correlation coefficient with 95% CI).

In G1L mice, the TDP-IR stage was positively correlated with life span (Spearman correlation coefficient with 95% CI, r = 0.77; 95% CI, 0.22–0.95) and negatively correlated with the formation of LBHIs (r = −0.87; 95% CI, −0.97 to −0.47). The correlation between life span and the number of LBHIs was also high (r = −0.64; 95% CI, −0.92 to 0.04). A cumulative probability plot of age at the end stage (Fig. 6) showed a higher value for the group with strong TDP-IR (Stages 3 and 4) than for those with weak TDP-IR (Stages 1 and 2); age at the end stage in the strong TDP-IR group was significantly greater than that in the weak TDP-IR group (Kolmogorov-Smirnov test, p = 0.015).

DISCUSSION

The TDP mislocalization from the nucleus to the cytoplasm was previously considered to be a disease-specific

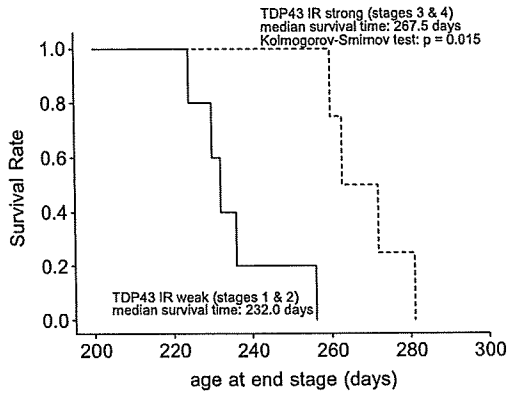

FIGURE 6. Kolmogorov-Smirnov test of the weak TAR DNA binding protein immunoreactivity (TDP-IR) groups (Stages 1 and 2) and strong TDP-IR groups (Stages 3 and 4) of G1L mice. Age at end stage in the TDP-IR strong group was significantly greater than that in the TDP-IR weak group ($p = 0.015$).

change not present in ALS1. Here, we analyzed TDP pathology in SALS and ALS1 patients and in ALS1 model mice. Our data suggest that the level of expression of TDP in the nucleus is associated with the clinical course and neurodegenerative changes in SALS patients and in ALS1 model mice.

Our observation that diffuse staining pattern was frequently observed in the cytoplasm of large neurons in SALS patients with rapid clinical courses showing mild neuronal loss suggests that TDP mislocalization starts gradually in the early phase of neurodegeneration. Most of the TDP-positive inclusions were found in atrophic neurons and glia, suggesting that the inclusions appeared later. Because no extracellular TDP-positive inclusions were apparent, neuronal TDP-positive inclusions likely disappear along with the death of the neurons.

In contrast, in SALS patients with slow clinical courses, no neurons with a diffuse TDP staining pattern in the cytoplasm were found, and TDP-positive inclusions in both neurons and glia were significantly less frequently found. Because relationships among the numbers of large neurons, those of TDP-positive inclusions in neurons, and those of TDP-positive inclusions in glia were not significant, the rarity of TDP pathology in SALS patients with a slow clinical course might not necessarily have resulted from severe neurodegeneration. The TDP pathology might be associated with a rapid clinical course in SALS. The influence of TDP-43 on the disease would then be less marked in SALS patients with a slow clinical course than in those with a rapid clinical course.

Previous studies have shown that LBHIs are not stained for TDP in ALS1 patients (16, 17, 26) and G1H mice (26).

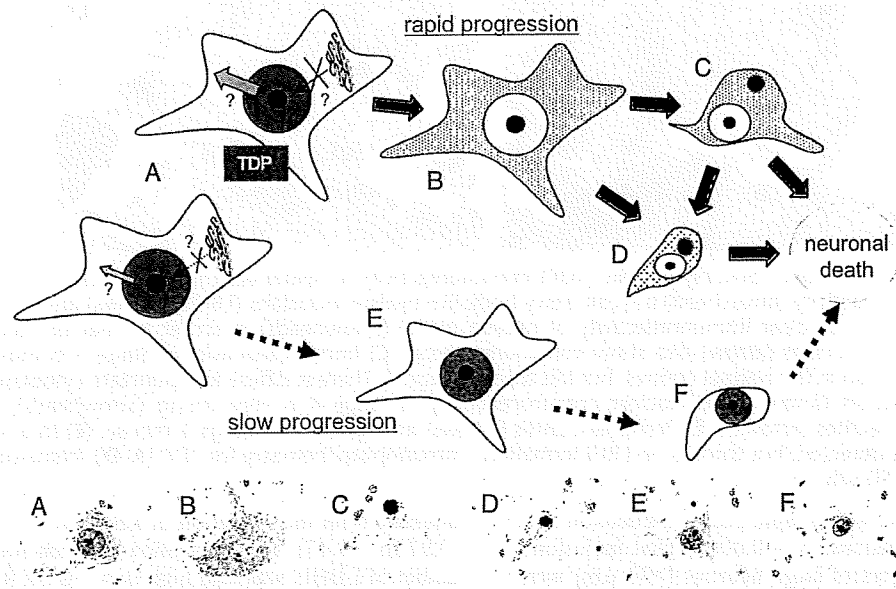

FIGURE 7. Hypothetical course of neuronal degeneration associated with changes in nuclear TAR DNA binding protein (TDP) expression in sporadic amyotrophic lateral sclerosis (SALS). **(A)** A morphologically normal neuron is subjected to an insult associated with a disturbance of TDP nuclear trafficking. The upper neuron diagrammed, from a patient with SALS, showing a rapid clinical course has marked disturbance of TDP nuclear trafficking, whereas the lower diagrammed neuron from a patient with SALS showing a slow clinical course, is only mildly affected. **(B–D)** Images show degenerating neurons at the time of rapid disease progression. **(B)** Early occurrence of TDP redistribution, i.e. low expression in nuclei and high expression in cytoplasm. **(C)** Later occurrence of cytoplasmic TDP aggregate in an atrophic neuron. **(D)** Similar aggregate of cytoplasmic TDP in a more degenerative neuron than that in **(C)**. **(E, F)** Images represent degenerative neurons at the time of slow disease progression. **(E)** Preservation of a high level of TDP expression in the nucleus of an atrophic neuron. **(F)** Successive maintenance of a high level of TDP expression in the nucleus of a more degenerative neuron. The lower 6 photographs are from SALS patients showing a rapid clinical course **(A–D)** and a slow course **(E, F)**, which correspond to the diagrammatic illustrations for each letter.

On the other hand, mislocalization of TDP to the cytoplasm in ALS1 cases (A4T, I113T) has been reported by Robertson et al (26). In the present study, TDP-positive LBHIs were clearly demonstrated in 1 ALS1 patient showing a slow disease progression, and in G1L mice, which also show slower disease progression than G1H mice. The ALS1 patients with TDP-negative LBHIs reported by Tan et al (17) showed very rapid progression within less than 1 year, and another ALS1 patient with TDP-negative LBHIs reported by Robertson et al (26) also showed rapid progression within 2 years. The difference in TDP immunoreactivity of LBHIs among ALS1 cases or between the 2 kinds of G93A mice might be a result of the difference in the clinical course or speed of SOD1 aggregation (34). The difference in morphology between TDP-positive inclusions in ALS1-1 and G1L mice and those in SALS patients would be caused by trapping of TDP-43 by SOD1 aggregation or LBHIs. The colocalization of TDP and SOD1 in LBHIs also suggests a biological relationship between SOD1 and TDP, although the specifics of that relationship are unclear.

Ayala et al (11) reported that loss of TDP in vitro results in nuclear dysmorphism, misregulation of the cell cycle, and apoptosis. Because the TDP-IR stage was positively correlated with life span in G1L mice, nuclei with low TDP-IR were atrophic and deformed in G1L mice and ALS1 patients, and an absence of TDP in the nucleus (such as that occurring through mislocalization) was frequently observed in SALS patients with a rapid clinical course, a high level of expression of nuclear TDP may play a protective role in neurons exposed to various insults. Because TDP-IR in the nucleus was inversely correlated with LBHI formation in G1L mice, TDP might have a suppressive effect on LBHI formation or toxic aggregation of SOD1, possibly through changes in the transcription and splicing of unknown genes (7, 8).

We hypothesized that rapid disease progression resulting from some insult to neurons might lead to disturbance of TDP nuclear trafficking (Fig. 7A) (35). Redistribution of TDP, with a low level of expression in the nucleus and a high level in the cytoplasm (Fig. 7B), occurs first, and cytoplasmic TDP later forms aggregates in the atrophic neurons (Figs. 7C, D). In contrast, neurons that succeed in maintaining a high level of expression of nuclear TDP (36) because of a slow shift of TDP (Fig. 7A, lower) show rather slower degeneration, and the disease progresses more slowly (Figs. 7E, F). It will be important to investigate the mechanism responsible for regulating the nuclear expression level of TDP, as this might yield a new strategy for treating not only ALS, but also other neurodegenerative disorders, including frontotemporal lobar degeneration.

ACKNOWLEDGMENTS

The authors thank T. Hamasaki and T. Sugimoto for their expert assistance with statistical analyses, and R. Yasui for technical assistance.

REFERENCES

1. Deng H-X, Hentati A, Tainer JA, et al. Amyotrophic lateral sclerosis and structural defects in Cu/Zn superoxide dismutase. Science 1993;261: 1047–51
2. Rosen DR, Siddique T, Patterson D, et al. Mutations in Cu/Zn superoxide dismutase gene are associated with familial amyotrophic lateral sclerosis. Nature 1993;362:59–62
3. Kato S. Amyotrophic lateral sclerosis models and human neuropathology: Similarities and differences. Acta Neuropathol 2008;115:97–114
4. Hadano S, Hand CK, Osuga H, et al. A gene encoding a putative GTPase regulator is mutated in familial amyotrophic lateral sclerosis 2. Nat Genet 2001;29:166–73
5. Yang Y, Hentati A, Deng HX, et al. The gene encoding alsin, a protein with three guanine-nucleotide exchange factor domains, is mutated in a form of recessive amyotrophic lateral sclerosis. Nat Genet 2001;29: 160–65
6. Buratti E, Brindisi A, Giombi M, et al. TDP-43 binds heterogenous nuclear ribonucleoprotein A/B through its C-terminal tail. J Biol Chem 2005;280:37572–84
7. Ayala YM, Pantano S, D'Ambrogio A, et al. Human, *Drosophila*, and *C. elegans* TDP43: Nucleic acid binding properties and splicing regulatory function. J Mol Biol 2005;348:575–88
8. Wang HY, Wang IF, Bose J, Shen CKJ. Structural diversity and functional implications of the eukaryotic *TDP* gene family. Genomics 2004;83:130–39
9. Buratti E, Baralle FE. Characterization and functional implications of the RNA binding properties of nuclear factor TDP-43, a novel splicing regulator of CFTR exon9. J Biol Chem 2001;276:36337–43
10. Mercado PA, Ayala YM, Romano M, et al. Depletion of TDP43 overrides the need for exonic and intronic splicing enhancers in the human apoA-II gene. Nucleic Acids Res 2005;33:6000–10
11. Ayala YM, Misteli T, Baralle FE. TDP-43 regulates retinoblastoma protein phosphorylation through the repression of cyclin-dependent kinase 6 expression. Proc Natl Acad Sci U S A 2008;105:3785–89
12. Kato S, Takikawa M, Nakashima K, et al. New consensus research on neuropathological aspects of familial amyotrophic lateral sclerosis with superoxide dismutase 1 (SOD1) gene mutations: Inclusions containing SOD1 in neurons and astrocytes. Amyotroph Lateral Scler Other Motor Neuron Disord 2000;1:163–84
13. Arai T, Hasegawa M, Akiyama H, et al. TDP-43 is a component of ubiquitin-positive tau-negative inclusions in frontotemporal lobar degeneration and amyotrophic lateral sclerosis. Biochem Biophys Res Commun 2006;351:602–11
14. Neumann M, Sampathu DM, Kwong LK, et al. Ubiquitinated TDP-43 in frontotemporal lobar degeneration and amyotrophic lateral sclerosis. Science 2006;314:130–33
15. Dickson DW, Josephs KA, Amador-Ortiz C. TDP-43 in differential diagnosis of motor neuron disorders. Acta Neuropathol 2007;114:71–79
16. Mackenzie IRA, Bigio EH, Ince PG, et al. Pathological TDP-43 distinguishes sporadic amyotrophic lateral sclerosis from amyotrophic lateral sclerosis with SOD1 mutations. Ann Neurol 2007;61:427–34
17. Tan C-F, Eguchi H, Tagawa A, et al. TDP-43 immunoreactivity in neuronal inclusions in familial amyotrophic lateral sclerosis with or without *SOD1* gene mutation. Acta Neuropathol 2007;113:535–42
18. Gitcho MA, Baloh RH, Chakraverty S, et al. TDP-43 A315T mutation in familial motor neuron disease. Ann Neurol 2008;63:535–38
19. Sreedharan J, Blair IP, Tripathi VB, et al. TDP-43 mutations in familial and sporadic amyotrophic lateral sclerosis. Science 2008;319: 1668–72
20. Cairns NJ, Neumann M, Bigio EH, et al. TDP-43 in familial and sporadic frontotemporal lobar degeneration with ubiquitin inclusions. Am J Pathol 2007;171:227–40
21. Amador-Ortiz C, Lin W-L, Ahmed Z, et al. TDP-43 immunoreactivity in hippocampal sclerosis and Alzheimer's disease. Ann Neurol 2007;6: 435–45
22. Nakashima-Yasuda H, Uryu K, Robinson J, et al. Co-morbidity of TDP-43 proteinopathy in Lewy body–related diseases. Acta Neuropathol 2007;114:221–29
23. Freeman SH, Spires-Jones TDP, Hyman BT, et al. TAR-DNA binding protein 43 in Pick disease. J Neuropathol Exp Neurol 2008;67:62–67
24. Lee EB, Lee M-Y, Trojanowski JQ, Neumann M. TDP-43 immunoreactivity in anoxic, ischemic and neoplastic lesions of the central nervous system. Acta Neuropathol 2007;115:305–11
25. Sanelli T, Xiao S, Horne P, et al. Evidence that TDP-43 is not the major ubiquitinated target within the pathological inclusions of amyotrophic lateral sclerosis. J Neuropathol Exp Neurol 2007;66:1147–53

26. Robertson J, Sanelli T, Xiao S, et al. Lack of TDP-43 abnormalities in mutant SOD1 transgenic mice shows disparity with ALS. Neurosci Lett 2007;420:128–32
27. Dal Canto MC, Gurney ME. A low expressor line of transgenic mice carrying a mutant *SOD1* gene develops pathological changes that most closely resemble those in human amyotrophic lateral sclerosis. Acta Neuropathol 1997;93:537–50
28. Parent A, Carpenter MB. *Carpenter's Human Neuroanatomy, 9th ed.* Philadelphia, PA: Lippincott, Williams &Wilkins, 1996
29. Sumi H, Nagano S, Fujimura H, et al. Inverse correlation between the formation of mitochondria-derived vacuoles and Lewy body–like hyaline inclusions in G93A superoxide dismutase–transgenic mice. Acta Neuropathol 2006;112:52–63
30. Kategawa J, Fujimura H, Ogawa Y, et al. A clinicopathological study of familial amyotrophic lateral sclerosis associated with two pair deletion in the copper/zinc superoxide dismutase (SOD1) gene. Acta Neuropathol (Berl) 1997;94:617–22
31. Kato S, Shimoda M, Watanabe Y, et al. Familial amyotrophic lateral sclerosis with a two base pair deletion in superoxide dismutase 1 (SOD1): Gene multisystem degeneration with intracytoplasmic hyaline inclusions in astrocytes. J Neuropathol Exp Neurol 1996;55:1089–101
32. Inoue K, Fujimura H, Ogawa Y, et al. Familial amyotrophic lateral sclerosis with a point mutation (G37R) of the superoxide dismutase 1 gene: A clinicopathological study. Amyotroph Lateral Scler Other Motor Neuron Disord 2002;3:244–47
33. Inoue K, Fujimura H, Toyooka K, et al. Familial amyotrophic sclerosis with L126S mutation of Cu/Zn superoxide dismutase gene. Pathological study of two cases [Abstract]. J Neurol 2006;235:120
34. Sato T, Nakanishi T, Yamamoto Y, et al. Rapid disease progression is correlated with instability of mutant SOD1 in familial ALS. Neurology 2006;65:1954–57
35. Winton MJ, Igaz LM, Wong MM, et al. Disturbance of nuclear and cytoplasmic Tar DNA binding protein (TDP-43) induces disease-like redistribution, sequestration and aggregate formation. J Biol Chem 2008; 283:13302–9
36. Wang IF, Chang HY, James Shen CK. TDP-43, the signature protein of FTLD-U, is a neuronal activity-responsive factor. J Neurochem 2008; 105:797–806

J Neuropathol Exp Neurol

Vol. 67, No. 11
November 2008
pp. 1063–1071

ORIGINAL ARTICLE

Nonviral DNA Vaccination Augments Microglial Phagocytosis of β-Amyloid Deposits as a Major Clearance Pathway in an Alzheimer Disease Mouse Model

Yoshio Okura, MD, PhD, Kuniko Kohyama, MS, Il-Kwon Park, DVM, PhD, and Yoh Matsumoto, MD, PhD

Abstract

Immunotherapies markedly reduce β-amyloid (Aβ) burden and reverse behavioral impairment in mouse models of Alzheimer disease. We previously showed that new Aβ DNA vaccines reduced Aβ deposits in Alzheimer disease model mice without detectable side effects. Although they are effective, the mechanisms of Aβ reduction by the DNA vaccines remain to be elucidated. Here, we analyzed vaccinated and control Alzheimer disease model mice from 4 months to 15 months of age to assess which of several proposed mechanisms may underlie the beneficial effects of this vaccination. Immunohistochemical analysis revealed that activated microglial numbers increased significantly in the brains of vaccinated mice after DNA vaccination both around Aβ plaques and in areas remote from them. Microglia in treated mice phagocytosed Aβ debris more frequently than they did in untreated mice. Although microglia had an activated morphological phenotype, they did not produce significant amounts of tumor necrosis factor. Amyloid plaque immunoreactivity and Aβ concentrations in plasma increased slightly in vaccinated mice compared with controls at 9 but not at 15 months of age. Collectively, these data suggest that phagocytosis of Aβ deposits by microglia plays a central role in Aβ reduction after DNA vaccination.

Key Words: β-Amyloid, Alzheimer disease, DNA vaccine, Microglia.

INTRODUCTION

Alzheimer disease (AD) is the most common cause of age-related cognitive decline; it affects more than 12 million people worldwide (1). It is widely believed that accumulation of β-amyloid (Aβ) is the first event in the pathogenesis of AD and that it precedes tau phosphorylation, tangle formation, and neuron death (i.e. the amyloid cascade hypothesis) (2). Based on this hypothesis, Schenk et al (3) demonstrated that a vaccine composed of synthetic Aβ in complete Freund adjuvant induced high anti-Aβ antibody titers, leading to dramatic reductions of Aβ deposits in platelet-derived growth factor promoter–expressing amyloid precursor protein (PDAPP) transgenic mice (3). On the basis of these promising results, clinical trials with Aβ peptide (AN-1792) in conjunction with the T helper 1 adjuvant, QS-21, were initiated; however, the clinical trial was halted because some patients developed meningoencephalitis (4). Importantly, neuropathologic examination of treated patients showed apparent clearance of Aβ plaques from large areas of the neocortex (5, 6). Thus, it seems that vaccine therapy could be effective for AD if inflammatory/immune reactions are minimized.

We previously developed nonviral Aβ DNA vaccines with plasmid vectors and succeeded in reducing Aβ burden in APP23 mice without inducing side effects such as neuroinflammation (7). The mechanism of Aβ reduction after DNA vaccination, however, has not yet been elucidated. Three hypotheses explain how anti-Aβ antibodies reduce Aβ deposits in the brain (8, 9). The first is that anti-Aβ antibodies attached to Aβ plaques enhance Fc receptor–mediated phagocytosis of Aβ by microglia (10). The second mechanism is the direct effect of antibodies on Aβ, leading to the dissolution of amyloid fibrils or neutralization of Aβ oligomers (11, 12). Finally, the "peripheral sink hypothesis" postulates that anti-Aβ antibodies in the circulation results in a net efflux of Aβ from the brain into blood vessels (13, 14).

In this study, we examined whether these clearance mechanisms take place in our DNA vaccination system. We found that microglia were activated, increased in number, and phagocytosed Aβ deposits after vaccine administration. The results suggest that phagocytosis of Aβ deposits by activated microglia is a major clearance pathway of Aβ clearance after DNA vaccination and may provide important information for the development of effective new vaccines against AD.

MATERIALS AND METHODS

Animals

APP23 transgenic and wild-type B6 mice were used for analysis; and detailed information was provided in a previous

From the Department of Molecular Neuropathology, Tokyo Metropolitan Institute for Neuroscience, Fuchu, Tokyo, Japan.
Send correspondence and reprint requests to: Yoh Matsumoto, MD, PhD, Department of Molecular Neuropathology, Tokyo Metropolitan Institute for Neuroscience, 2-6 Musashidai, Fuchu, Tokyo, Japan 183-8526; E-mail: matyoh@tmin.ac.jp
This study was supported in part by Health and Labour Sciences Research Grants for Research on Psychiatric and Neurological Diseases and Mental Health and by Grants-in-Aid from the Japan Society for the Promotion of Science. Yoh Matsumoto was also supported by the Welfare and Health Fund of the Tokyo Metropolitan Government.

report (7). Plasma was obtained from mice under deep inhalation anesthesia with ethyl ether via cardiac puncture with heparinized syringes before autopsy. Anesthetized mice were then killed. All procedures of animal experimentation were approved by the ethics committee of the Tokyo Metropolitan Institute for Neuroscience and performed in accordance with institutional guidelines.

Development and Administration of DNA Vaccines

We prepared Aβ DNA vaccines using a PTarget mammalian expression system (Promega, Tokyo, Japan) and injected them into APP23 mice on a weekly and then biweekly basis as used previously (15). Two DNA vaccines were used: immunoglobulin L (IgL)–Aβ vaccine, which possesses the Igκ signal sequence of mouse immunoglobulin to improve the secretion ability, and Aβ-Fc vaccine that has the Fc portion of human immunoglobulin at the 3′ end to maintain stability. APP23 mice received DNA vaccines (100 μg in 100 μL) regularly from 4 months of age, 2 months before amyloid plaque appearance, to the termination of experiments. Mice were killed at 9 and 15 months of age.

Immunohistochemistry

Mice were killed under deep anesthesia, and the brains were removed and immersion fixed in 4% paraformaldehyde. Paraffin-embedded sections were stained with monoclonal antibodies (mAbs) 6F/3D against Aβ8-17 (DAKO, Tokyo, Japan) and Iba-1 for microglia (WAKO, Tokyo, Japan). Sections were pretreated in formic acid for 3 minutes for 6F/3D staining and 0.1% trypsin for 10 minutes at 37°C for Iba-1 staining. After pretreatment, the sections were incubated in the primary mAbs followed by biotinylated horse anti-mouse immunoglobulin G (IgG) and horseradish peroxidase (HRP)–labeled Vectastain Elite ABC kit (Vector, Funakoshi, Tokyo, Japan). Horseradish peroxidase–binding sites were detected in 0.005% diaminobenzidine and 0.01% hydrogen peroxide. For confocal microscopic analysis, fluorescein isothiocyanate anti-mouse IgG and Cy-3 anti-rabbit IgG were used as secondary antibodies for 6F/3D and Iba-1 staining, respectively. The presence or absence of IgG depositions on Aβ plaques was determined by incubation of sections with biotinylated horse anti-mouse IgG followed by HRP-labeled Vectastain Elite ABC kit.

Quantitative Analysis of Aβ Burden and Microglia

β-Amyloid deposits were quantitated in the cerebral cortex and hippocampus according to the method used previously (15). All the procedures were performed by an individual blinded to the experimental conditions. The amyloid load was measured in 10 fields from the cingulate to retrosplenial cortex in the left hemisphere per mouse. Each field measured 600 × 400 μm and was randomly chosen. Analysis of the entire hippocampus was performed in a similar manner. β-Amyloid deposits that occupied the field were expressed as pixels using National Institutes of Health (NIH) image software.

After Iba-1 staining, the densities of microglia were determined by counting them in randomly selected 10 fields (600 × 400 μm each) from the cingulate to retrosplenial cortex in the left hemisphere of mice (n = 4–6 in each group). Microglia around the plaque (periplaque area) and those remote from the plaque (remote area) were counted separately and expressed as the mean ± SE per field. Using double-stained sections for Aβ and microglia, the densities of phagocytosing microglia were determined in a similar manner under confocal microscopy.

Western Blotting

Brain tissues were homogenized and sonicated in 10 volumes of Tris-buffered saline buffer in the presence of protease inhibitors. One milliliter of formic acid was added to 300 μg of homogenate in 10 μL. After a brief incubation, formic acid was vacuum dried with an acid-proof vacuum evaporator (miVac DNA, Scrum, Tokyo, Japan). After adding NuPAGE LDS sample buffer (Invitrogen, Tokyo, Japan), the samples were incubated at 70°C for 10 minutes and were run on NuPAGE 12% Bis-Tris gel (Invitrogen) (16). Before electrophoresis, protein concentration of each sample was determined, and the volume for loading was adjusted (equivalent to 40 μg); samples were then transferred to polyvinylidene difluoride membrane (Immobilon-P; Millipore, Tokyo, Japan). After blocking with 10% nonfat milk, the blots were incubated with anti-human Aβ 1–17 antibody (6E10; Cambridge, United Kingdom; 1:100) at 4°C overnight followed by incubation with Trueblot HRP-conjugated anti-mouse IgG (eBioscience, San Diego, CA; 1:1000) for 1 hour. The blots were developed by enhanced chemiluminescence reagents (Immunostar Kit Wako; WAKO) according to the manufacturer's instructions. The density of each band obtained by Western blot analysis was measured with a scanning laser densitometer (GS-700, Bio-Rad, Hercules, CA) and analyzed using the NIH image software.

Real-time Polymerase Chain Reaction

Total RNA was extracted from the indicated tissues using an RNAqueous Kit (Ambion), and complementary DNA was then synthesized by reverse transcription using a High Capacity cDNA Reverse Transcription Kit (Applied Biosystems, Foster City, CA). SYBR Green real-time polymerase chain reactions (PCRs) were performed on an ABI PRISM 7500 sequence detection system (Applied Biosystems) in a total volume of 25 μL using the SYBR Premix Ex Taq (Takara Bio, Otsu, Japan). Each PCR was performed in duplicate using thermocycler conditions: Stage 1, 95°C for 10 minutes for 1 cycle and Stage 2, 95°C for 15 seconds and 58°C for 1 minute for 50 cycles. All primers were designed on an intron-exon junction to prevent coamplification of genomic DNA, and their sequences were shown in previous reports (17, 18). Relative quantification of messenger RNA (mRNA) was performed using the standard curve method. Glyceraldehyde-3-phosphate dehydrogenase was used as internal control. The absence of nonspecific amplification was confirmed by dissociation curve analysis.

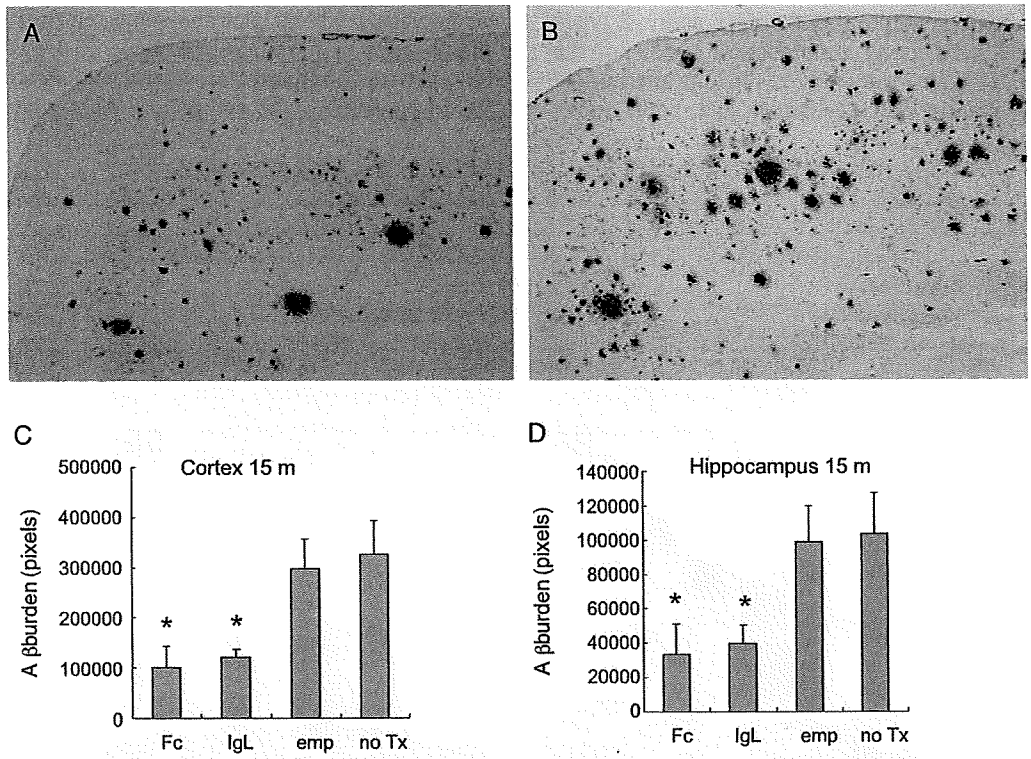

FIGURE 1. β-Amyloid (Aβ) reduction after DNA vaccination in mice at 15 months of age. There were fewer Aβ deposits in the frontal cortex of a mouse that had been treated with the Aβ-Fc vaccine **(A)** than in frontal cortex of a control mouse **(B)**. Semiquantitative analysis revealed that Aβ deposits were significantly reduced (* = $p < 0.01$) in the cortex of vaccinated mice (30.6% of untreated mice) **(C)**. β-Amyloid deposits in the hippocampus were also significantly reduced (* = $p < 0.01$) after vaccine treatment **(D)**. emp, empty vector; no Tx, untreated.

Tissue Amyloid Plaque Immunoreactivity Assay

Plasma to be tested were diluted to ×100, ×300, ×1,000, and ×3,000, and then applied to formic acid-pretreated APP23 brain sections, followed by incubation with biotinylated horse anti-mouse IgG and HRP-labeled Vectastain Elite ABC kit (Vector). The maximal dilution of plasma that gave positive staining was estimated as the amyloid plaque immunoreactivity titer.

Quantification of Tumor Necrosis Factor in the CNS Tissues and Plasma Aβ With ELISA

Brain tissue was homogenized in lysis buffer, and the supernatant was harvested after centrifugation. Each sample was adjusted to 10 mg/mL. The levels of brain tumor necrosis factor (TNF) and plasma Aβ were determined using the Mouse TNF Instant ELISA (Bender MedSystems, Vienna, Austria) and human Aβ (1–42) ELISA Kit (WAKO),

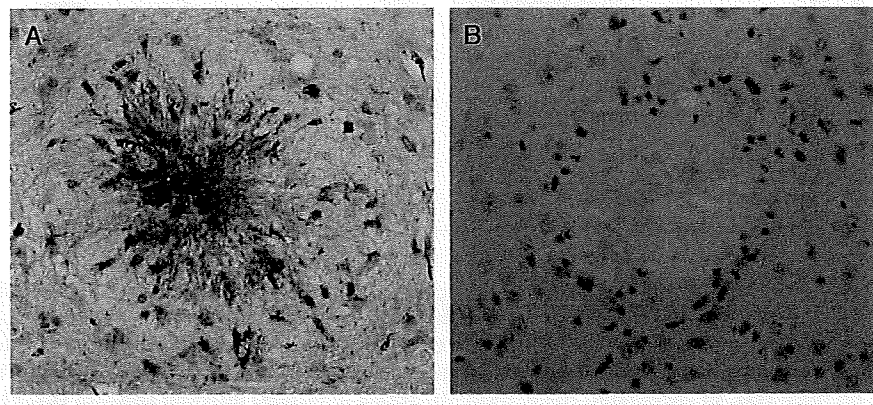

FIGURE 2. Immunoglobulin G (IgG) in the brains of DNA vaccine–treated and untreated APP23 mice at age 15 months. β-Amyloid (Aβ) plaques in the brain of an Aβ-Fc vaccine–treated mouse stained positively for IgG **(A)**, whereas a plaque in an untreated mouse was completely negative **(B)**. Immunohistochemistry with anti-mouse IgG. Original magnification: 200×.

respectively. For positive controls in the TNF assay, 2 types of brain and spinal cord tissue samples were used. For the first type, C57Bl6 mice were given an intraperitoneal injection of 100 μg lipopolysaccharide, and brain tissue was harvested 1 hour later and subjected to ELISA. Second, C57Bl6 mice were immunized twice on Days 0 and 7 with 300 μg of recombinant rat myelin oligodendrocyte protein (MOG) emulsified with complete Freund adjuvant. On Days

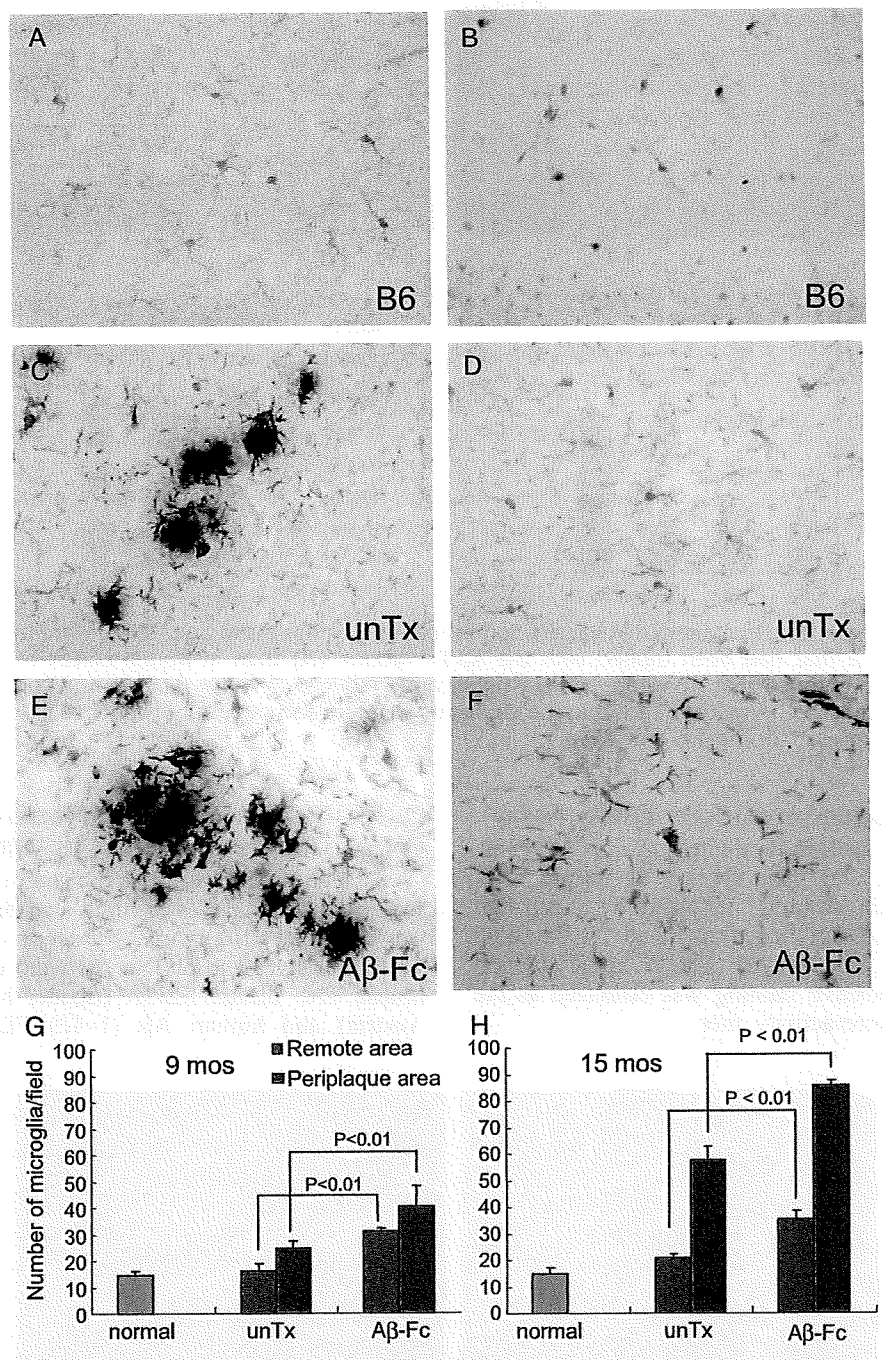

FIGURE 3. Double staining with monoclonal antibodies 6F3D against β-amyloid (Aβ) (blue) and Iba-1 against microglia (brown) of the brains of treated and untreated mice. In normal control B6 mice, ramified resting microglia were sparse in the cortex **(A)** and hippocampus **(B)**. Around plaques of untreated APP23 mice, there were microglia with abundant cytoplasm and processes that had bulbous swellings **(C)**. In areas remote from the plaques in nontreated APP23 mice, resting microglia were sparsely distributed as in control B6 mice **(D)**. In vaccinated mice, more microglia infiltrated amyloid plaques **(E)**. In the area remote from plaques in treated APP23 mice, microglia were more numerous and showed an activated phenotype **(F)**. Semiquantitative analysis was performed at 9 months **(G)** and 15 months **(H)** by counting microglial cell number in 10 fields (3–4 mice per group). Normal, normal B6 mice; unTx, untreated APP23 mice; Aβ-Fc, vaccinated mice.

0 and 2, the mice received intraperitoneal injection of pertussis toxin (300 ng). When they showed complete hind leg paralysis on Day 20 (i.e. clinical experimental autoimmune encephalomyelitis [EAE]), lumbar spinal cords were removed and subject to ELISA analysis.

Statistical Analysis

Student *t*-test or the Mann-Whitney U test was used for the statistical analysis. Values of $p < 0.05$ were considered significant.

RESULTS

DNA Vaccination Reduces Aβ Burden in the Brains of AD Model Mice

We prepared nonviral Aβ DNA vaccines and injected them (100 μg each) into APP23 mice beginning at 4 months of age on a weekly and then biweekly basis (7). At 15 months of age, Aβ deposits were considerably reduced (Figs. 1A, B). Semiquantitative analysis revealed that Aβ deposits in treated mice were reduced to approximately one third of those in nonvaccinated control mice in both the cerebral cortex and hippocampus (Figs. 1C, D).

IgG Deposits Were Detected on Aβ Plaques in the Brains of DNA-Vaccinated, But Not Control Mice

To determine the possible mechanisms of Aβ reduction after DNA vaccination, it was essential to know whether the anti-Aβ antibodies raised by vaccination reach the brain and decorate Aβ plaques. We previously found that the DNA vaccination protocol resulted in a mild but significant induction of anti-Aβ antibodies in plasma in vaccinated mice (7). We performed immunohistochemistry using anti-mouse IgG antibodies to identify IgG on Aβ plaques. Plaques in the brains of treated mice were stained positively for IgG (Fig. 2A), whereas those in untreated mice were completely negative (Fig. 2B). Some cells with morphological features of microglia were also positive for IgG (Fig. 2A). Interestingly, Aβ plaques in empty vector–administered mice were also negative for IgG (data not shown). Thus, antibody binding to the Aβ plaques may occur in the brains of vaccinated mice in vivo.

Microglial Activation and Phagocytosis Induced by DNA Vaccination

We assessed phagocytosis of Aβ deposits by microglia after DNA vaccination. Brain sections from treated and control (i.e. untreated APP23 and wild-type) mice were double-stained with Iba-1 and 6F/3D mAbs. We previously determined that DNA vaccination did not elicit neuroinflammation in either AD model or wild-type mice (7). Because in the present study, Iba-1–positive cells in the CNS showed typical features of resident microglia, they likely were microglia and not macrophages. In untreated B6 mice, ramified microglia with small cytoplasm and fine processes were sparsely distributed throughout the cerebral cortex

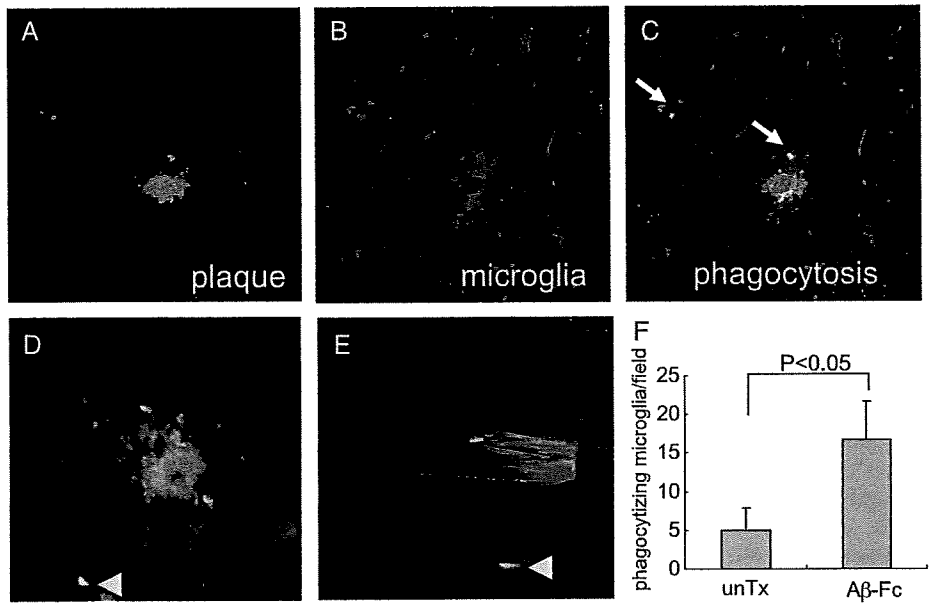

FIGURE 4. Phagocytosis of β-amyloid (Aβ) deposits by activated microglia in the cerebral cortex of mice at 15 months of age. Brain sections from treated **(A–E)** and untreated (not shown) APP23 mice were stained for Aβ with (6F3D, green) **(A)** and for microglia (Iba-1, red) **(B)** monoclonal antibodies and observed with a confocal microscope. Some microglia surrounding the amyloid plaque contained Aβ deposits (C, arrows). Microglia (red) in areas away from Aβ plaques had Aβ staining (**D**, arrowhead) within the cytoplasm. Using 3-dimensional reconstruction, a different plane of the view was shown in (**E**). The Aβ deposit ingested by a microglial cell was indicated by an arrowhead in **(E)**. Semiquantitative analysis revealed that the number of phagocytosed Aβ deposits increased approximately 2.5-fold in treated compared with untreated mice ([**F**] $p < 0.05$). Phagocytosed particles in 10 fields from 4 treated and 4 control mice (total, 40 fields in each group) were counted and compared.

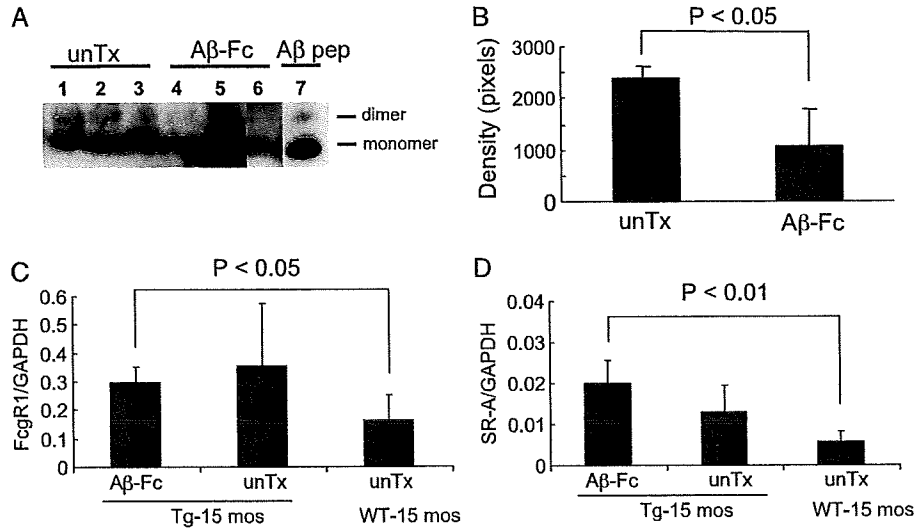

FIGURE 5. Western blot analysis **(A)** demonstrated that β-amyloid (Aβ) monomers plus dimers were reduced after DNA vaccination. Measurements of band densities revealed a statistically significant difference between vaccinated and control samples ($p < 0.05$). Lanes 1 to 5 and 7 were obtained from the same blot. Although Lane 6 was from a different blot, it was confirmed that the densities of the standard synthetic peptide in 2 blots were identical. unTx, untreated APP23 mice; Aβ-Fc, vaccinated mice; Aβ-pep, synthetic Aβ peptide positive control. **(C, D)** Real-time polymerase chain reaction analysis of messenger RNA (mRNA) levels of phagocytosis-related receptors, Fcγ receptor 1 (FcγR1) and scavenger receptor A (SR-A). Messenger RNA for these receptors was significantly greater in vaccinated APP mice than in untreated wild-type mice. Receptor mRNAs were also upregulated in untreated APP mice, consistent with the observations that microglia were activated and increased in untreated APP mice (Fig. 3). There were no significant differences between vaccinated and untreated APP mice or between untreated APP and wild-type mice in **(C)** and **(D)**. GAPDH, glyceraldehyde-3-phosphate dehydrogenase.

(Fig. 3A) and hippocampus (Fig. 3B). In untreated APP23 transgenic mice, activated ameboid microglia were seen around amyloid plaques (periplaque area); their processes were present deep within the plaques (Fig. 3C). In areas away from the plaques (remote area), ramified microglia were similar to those in wild-type mice (Fig. 3D). After DNA vaccination, microglia in the periplaque area seem to be increased in number and were clustered around the plaques (Fig. 3E). The major difference between vaccinated and nonvaccinated AD mice, however, was the morphological change of microglia in the remote areas. In vaccinated mice, microglia had more ameboid forms with long processes (Fig. 3F). To analyze the increase of microglia in a semi-quantitative manner, microglia were counted in both periplaque and remote areas in brain sections from normal, untreated, and treated mice. At 9 months of age, there were significantly more microglia in both areas in treated compared with untreated AD mice ($p < 0.01$); in treated mice, microglia were more numerous in periplaque areas (40.3 ± 7.9 in each 600 × 400 μm field) compared with remote areas (30.9 ± 2.7 in each field; Fig. 3G). At 15 months of age, immunostained microglia were also more numerous, particularly in periplaque areas in AD mice, with patterns similar to those at 9 months of age (Fig. 3H).

In double-stained brain sections, small Aβ deposits seemed to be located inside microglia. This was confirmed by confocal microscopy. In periplaque area, Cy3-labeled microglia (red) (Fig. 4B) enclosed fluorescein isothiocyanate–labeled Aβ deposits (green) (Fig. 4A). The merged image indicates small Aβ deposits within microglia (arrows in Fig. 4C). Ingestion of Aβ deposits was confirmed by 3-dimensional reconstruction view. Localization of Aβ deposits within the cytoplasm of microglia was demonstrated by the

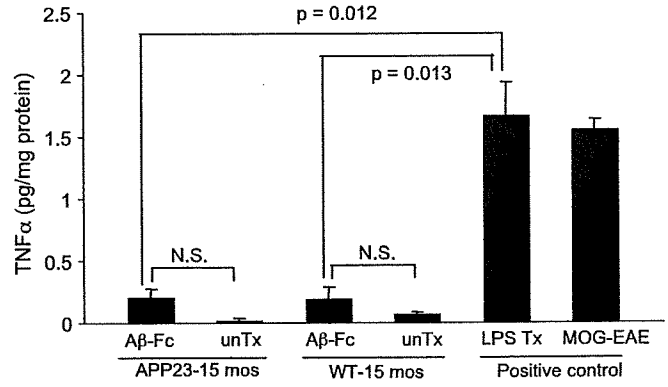

FIGURE 6. Tumor necrosis factor (TNF) levels in the brains of β-amyloid (Aβ)-Fc–treated and untreated B6 and APP23 mice detected by ELISA of CNS tissue homogenates. Large amounts of TNF were detected in the brains of positive control mice that had been given either an intraperitoneal injection of lipopolysaccharide or myelin oligodendrocyte protein (MOG)–induced experimental autoimmune encephalomyelitis ([EAE] spinal cord sample). Tumor necrosis factor in the brains of untreated B6 and APP23 mice was almost undetectable. p values are indicated. Additional p values for Aβ-Fc APP23 versus MOG-EAE and Aβ-Fc wild-type versus MOG-EAE are $p = 0.0001$ and $p = 0003$, respectively. Aβ-Fc, vaccinated mice; unTx, untreated APP23 mice.

different plane of the z axis view (Figs. 4D, E). Semi-quantitative analysis revealed that the numbers of microglia phagocytosing Aβ deposits were significantly increased in vaccine-treated compared with untreated mice ($p < 0.05$; Fig. 4F). Phagocytosis in remote areas was interpreted as indicating clearance of invisible small Aβ aggregates such as Aβ oligomers by activated microglia.

To confirm this, we performed Western blot analysis. As shown in Figures 5A and B, Aβ aggregates were reduced by DNA vaccination compared with untreated controls. Thus, Aβ phagocytosis away from amyloid plaques and Aβ oligomer reduction after DNA vaccination may be beneficial for cognitive decline in AD patients because Aβ oligomers show toxic effects on neurons in AD brains (19, 20). We also quantitated mRNA levels of phagocytosis-related receptors, Fcγ receptor 1 and scavenger receptor A, by real-time PCR. As shown in Figures 5C and D, mRNA for these receptors was significantly upregulated in vaccinated APP mice compared with untreated wild-type mice. However, receptor mRNA was also upregulated in untreated APP mice. This finding was consistent with morphological observations that microglia were activated and increased in untreated APP mice (Fig. 3).

TNF Did Not Increase Significantly in the Brain After DNA Vaccination

To determine whether activated microglia in AD mice are neurotoxic or neuroprotective, we measured the TNF levels with ELISA. Tumor necrosis factor is a proinflammatory cytokine and is regarded as a biomarker of risk for the development of meningoencephalitis (21). Large amounts of TNF were detected in the brains of LPS-treated mice and in the spinal cords of mice with MOG-induced EAE, but levels of TNF in the brain of vaccinated and control B6 and APP23 mice assayed in the same manner were very low (Fig. 6). Thus, activated microglia in the brains of DNA vaccinated AD model mice did not produce large amounts of TNF and seem to be nonneurotoxic.

Direct Effects of Anti-Aβ Antibodies on Aβ Plaques as Suggested by Amyloid Plaque Immunoreactivity Assay

The second hypothesis to explain the mechanism of Aβ reduction is the direct effect of anti-Aβ antibodies on Aβ deposits, leading to the dissolution of amyloid fibrils or neutralization of Aβ oligomers (22). Because it was difficult

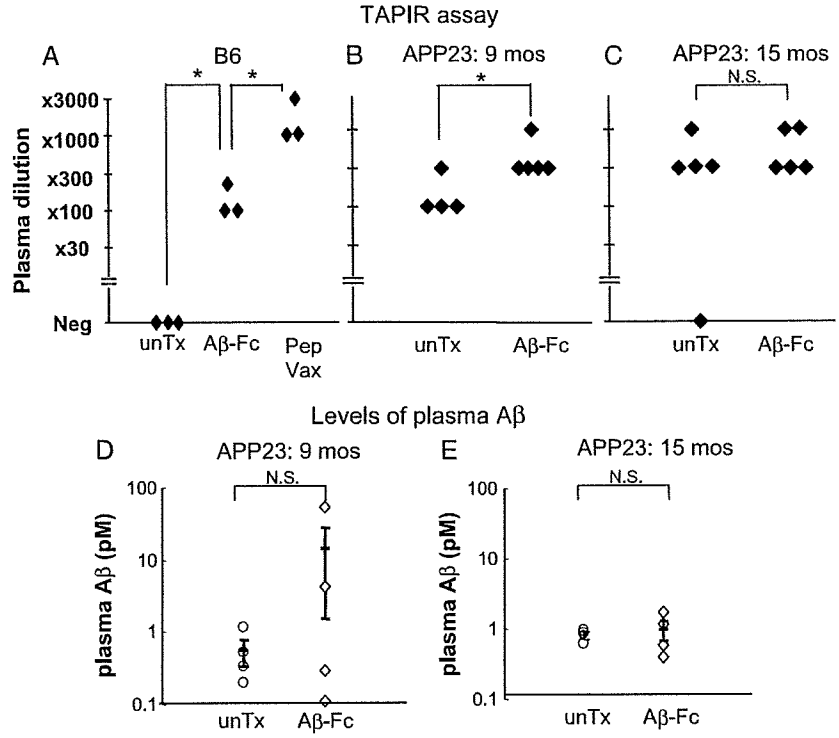

FIGURE 7. Tissue amyloid plaque immunoreactivity (TAPIR) assay and plasma β-amyloid (Aβ) levels in DNA vaccinated and untreated mice. **(A–C)** The binding of plasma from Aβ-immunized mice to Aβ plaques was determined using the TAPIR assay. **(A)** In plasma from untreated B6 mice, there was no Aβ-binding activity (unTx). By contrast, plasma from Aβ peptide–immunized B6 mice (Pep Vax) showed high titers, and plasma from DNA-vaccinated mice (DNA Vax) showed intermediate values. Asterisks indicate $p < 0.05$. **(B)** Plasma from untreated APP23 mice at 9 months of age showed intermediate binding, which was significantly different from the treated group ($p < 0.05$); differences were not significant (N.S.) at 15 months of age **(C)**. **(D, E)** At 9 months of age, plasma Aβ levels were slightly increased in some mice after DNA vaccine therapy **(D)**, but at 15 months of age, plasma Aβ levels in treated mice were almost the same as those of untreated mice **(E)**. No differences between treated and untreated groups at either age were significant (N.S.). unTx, untreated APP23 mice; Aβ-Fc, vaccinated mice.

to estimate the direct effects in vivo, we measured Aβ-binding activities of plasma from treated and untreated mice using a tissue amyloid plaque immunoreactivity assay on sections from APP23 mice. First, we determined the plaque-binding ability of plasma taken from nonimmunized and immunized B6 mice (Fig. 7A). Plasma samples from non-immunized mice did not show detectable levels of amyloid plaque immunoreactivity activities, whereas samples from Aβ peptide–immunized mice showed significantly higher levels. Plasma from DNA vaccine–injected mice showed intermediate levels (Fig. 7A). The binding activity of plasma from vaccinated APP23 mice was significantly higher than that from untreated APP23 mice at 9, but not at 15, months of age (Figs. 7B, C). It should be noted that amyloid plaque immunoreactivity activities of plasma of untreated APP23 mice were elevated, especially at 15 months. This may correspond to elevation of the plasma antibody titer of untreated model mice as previously reported (7). The Aβ plaques were, however, negative for IgG in these mice (Fig. 2B). Collectively, these findings indicate that the binding activities of anti-Aβ antibodies to Aβ were augmented by DNA vaccination at early stages of the disease, but that the direct effects of antibodies are not as strong at later stages.

Plasma Aβ Levels in Vaccinated and Untreated Mice

We next measured the levels of plasma Aβ peptide to evaluate the so-called sink effect by blood-circulating anti-Aβ antibodies. At 9 months of age, plasma Aβ was slightly elevated in some cases after vaccine treatment (Fig. 7D). At 15 months of age, the levels of plasma Aβ in the treated group were almost the same as those in the untreated group (Fig. 7E). These findings suggest that Aβ efflux from the brain to blood (i.e. "peripheral sink") is present in some treated mice at an early stage, but does not seem to be the major route of Aβ reduction after DNA vaccination.

DISCUSSION

Immunotherapies against AD are effective not only in the mouse model (3, 23), but also in human clinical trials (5); however, the mechanisms by which raised or transferred anti-Aβ antibodies reduce Aβ deposition in the brain remain to be elucidated. We examined 3 possible Aβ reduction mechanisms to determine the major route of Aβ clearance in our DNA vaccination system and found that DNA vaccination enhances the phagocytosis of Aβ deposits by microglia. Because Aβ plaques in the brains of vaccinated, but not of empty vector–administered and untreated mice, were positive for IgG, an IgG-mediated immune-mediated mechanism such as Fc-mediated phagocytosis of Aβ by microglia may take place after DNA vaccination. Although it has been reported that Aβ reduction by activated microglia after glatiramer acetate treatment was achieved without the involvement of anti-Aβ antibodies (24, 25), we believe that the antibodies play an essential role in microglial activation in our DNA vaccination system. This was because plasmid DNAs containing the CpG motif without the Aβ sequence (i.e. empty vector) were not effective in Aβ reduction (Fig. 1). Increase of plaque-binding properties of plasma in vaccinated mice at 9 months of age also suggested the presence of anti-Aβ antibodies on Aβ plaques. There was, however, no significant difference in this activity between the treated and untreated groups at 15 months of age. Sink effects of plasma anti-Aβ antibodies may be present at the early stage in some treated mice but become unclear at later stages. There are at least 2 explanations for these results. First, anti-Aβ antibodies in plasma were only mildly elevated after DNA vaccination (7). Second, cerebral amyloid angiopathy may progress, especially in the late stage, and interfere with the perivascular drainage pathway of Aβ (26). Thus, microglial activation and their subsequent enhanced phagocytosis of Aβ deposits is a major Aβ clearance pathway in DNA vaccine therapy. Importantly, DNA vaccination reduced not only visible Aβ deposits, but also Aβ oligomers (Fig. 5). Thus, the findings obtained in this study provide useful information for the development of new and more effective DNA vaccines against AD.

There have been some controversies with regard to the role of microglia in AD pathogenesis. Previously, microglia were thought to be harmful and toxic to neurons in the AD brain because there were sustained inflammatory responses, including complement activation (27). β-Amyloid plaques and interferon-γ–activated microglia have synergistic effects on neuronal degeneration, which may have a role in the pathogenesis of aging and AD (28). Upon activation, microglia are known to secrete a wide variety of molecules involved in inflammation, many of which are potentially neurotoxic (29). It has been shown, however, that microglia react with Aβ plaques and phagocytose Aβ deposits under various conditions (30–33). Furthermore, activated microglia may play a protective role in the brain through the secretion of neurotrophic factors and cytokines (34). In the present study, we demonstrated that DNA vaccination induced microglial activation and augmentation of phagocytosis but did not induce large amounts of TNF production in the brains of vaccinated APP23 mice. We therefore speculate that only microglia attached to Aβ plaques may secrete TNF locally, which does not influence the level of TNF detected by ELISA, and this is less likely because microglial activation was diffuse in both periplaque and remote areas. These findings suggest that microglia after DNA vaccination may in part be neuroprotective in AD.

Increasing evidence suggests that microglia do not constitute a single uniform cell population, but rather a family of cells with diverse phenotypes—some that are beneficial and others that are destructive (35). Proper regulation of inflammatory responses to injury will arrest degeneration and promote regrowth, whereas inappropriate regulation will lead to ongoing degeneration (36). Microglial differentiation, neuroprotective or neurotoxic, might be determined by the strength of the stimulus.

The success of vaccine therapies depends on how to control microglial function to obtain beneficial effects in the AD brain. From this standpoint, DNA vaccination has advantages over other immunotherapies. The constructs of DNA vaccines can be easily manipulated by adding appropriate additional sequences to control microglial functions. Moreover, DNA vaccines may be safer because their half-life

within the body is shorter than those of others (37). If adverse side effects occur, they can be easily controlled by stopping further administration of the vaccine. Therefore, DNA vaccination may be a promising therapy for AD in the near future.

ACKNOWLEDGMENT

The authors thank Dr Matthias Staufenbiel of Novartis Institute of Biomedical Research, Nervous System, Switzerland, for critical reading of the manuscript.

REFERENCES

1. Citron M. Alzheimer's disease: Treatments in discovery and development. Nat Neurosci 2002;(suppl 5):1055–57
2. Hardy J, Allsop D. Amyloid deposition as the central event in the aetiology of Alzheimer's disease. Trends Pharmacol Sci 1991;12:383–88
3. Schenk D, Barbour R, Dunn W, et al. Immunization with amyloid-beta attenuates Alzheimer-disease-like pathology in the PDAPP mouse. Nature 1999;400:173–77
4. Orgogozo JM, Gilman S, Dartigues JF, et al. Subacute meningoencephalitis in a subset of patients with AD after Abeta42 immunization. Neurology 2003;61:46–54
5. Nicoll JA, Wilkinson D, Holmes C, Steart P, Markham H, Weller RO. Neuropathology of human Alzheimer disease after immunization with amyloid-beta peptide: A case report. Nat Med 2003;9:448–52
6. Ferrer I, Boada Rovira M, Sanchez Guerra ML, Rey MJ, Costa-Jussa F. Neuropathology and pathogenesis of encephalitis following amyloid-beta immunization in Alzheimer's disease. Brain Pathol 2004;14:11–20
7. Okura Y, Miyakoshi A, Kohyama K, Park IK, Staufenbiel M, Matsumoto Y. Nonviral Abeta DNA vaccine therapy against Alzheimer's disease: Long-term effects and safety. Proc Natl Acad Sci U S A 2006;103:9619–24
8. Morgan D. Mechanisms of A beta plaque clearance following passive A beta immunization. Neurodegener Dis 2005;2:261–66
9. Morgan D. Immunotherapy for Alzheimer's disease. J Alzheimers Dis 2006;9:425–32
10. Bard F, Barbour R, Cannon C, et al. Epitope and isotype specificities of antibodies to beta-amyloid peptide for protection against Alzheimer's disease–like neuropathology. Proc Natl Acad Sci U S A 2003;100:2023–28
11. Bacskai BJ, Kajdasz ST, McLellan ME, et al. Non-Fc–mediated mechanisms are involved in clearance of amyloid-beta in vivo by immunotherapy. J Neurosci 2002;22:7873–78
12. Solomon B, Koppel R, Frankel D, Hanan-Aharon E. Disaggregation of Alzheimer beta-amyloid by site-directed mAb. Proc Natl Acad Sci U S A 1997;94:4109–12
13. DeMattos RB, Bales KR, Cummins DJ, Dodart JC, Paul SM, Holtzman DM. Peripheral anti-A beta antibody alters CNS and plasma A beta clearance and decreases brain A beta burden in a mouse model of Alzheimer's disease. Proc Natl Acad Sci U S A 2001;98:8850–55
14. Dodart JC, Bales KR, Gannon KS, et al. Immunization reverses memory deficits without reducing brain Abeta burden in Alzheimer's disease model. Nat Neurosci 2002;5:452–57
15. Sigurdsson EM, Scholtzova H, Mehta PD, Frangione B, Wisniewski T. Immunization with a nontoxic/nonfibrillar amyloid-beta homologous peptide reduces Alzheimer's disease–associated pathology in transgenic mice. Am J Pathol 2001;159:439–47
16. Fonte J, Miklossy J, Atwood C, Martins R. The severity of cortical Alzheimer's type changes is positively correlated with increased amyloid-beta levels: Resolubilization of amyloid-beta with transition metal ion chelators. J Alzheimers Dis 2001;3:209–19
17. Matsumoto Y, Tsukada Y, Miyakoshi A, Sakuma H, Kohyama K. C protein–induced myocarditis and subsequent dilated cardiomyopathy: Rescue from death and prevention of dilated cardiomyopathy by chemokine receptor DNA therapy. J Immunol 2004;173:3535–41
18. Matsumoto Y, Sakuma H, Miyakoshi A, et al. Characterization of relapsing autoimmune encephalomyelitis and its treatment with decoy chemokine receptor gene. J Neuroimmunol 2005;170:49–61
19. Bucciantini M, Calloni G, Chiti F, et al. Prefibrillar amyloid protein aggregates share common features of cytotoxicity. J Biol Chem 2004;279:31374–82
20. Bucciantini M, Giannoni E, Chiti F, et al. Inherent toxicity of aggregates implies a common mechanism for protein misfolding diseases. Nature 2002;416:507–11
21. O'Toole M, Janszen DB, Slonim DK, et al. Risk factors associated with beta-amyloid (1-42) immunotherapy in preimmunization gene expression patterns of blood cells. Arch Neurol 2005;62:1531–36
22. Kotilinek LA, Bacskai B, Westerman M, et al. Reversible memory loss in a mouse transgenic model of Alzheimer's disease. J Neurosci 2002;22:6331–35
23. Janus C, Pearson J, McLaurin J, et al. A beta peptide immunization reduces behavioural impairment and plaques in a model of Alzheimer's disease. Nature 2000;408:979–82
24. Frenkel D, Maron R, Burt DS, Weiner HL. Nasal vaccination with a proteosome-based adjuvant and glatiramer acetate clears beta-amyloid in a mouse model of Alzheimer disease. J Clin Invest 2005;115:2423–33
25. Butovsky O, Koronyo-Hamaoui M, Kunis G, et al. Glatiramer acetate fights against Alzheimer's disease by inducing dendritic-like microglia expressing insulin-like growth factor 1. Proc Natl Acad Sci U S A 2006;103:11784–89
26. Weller RO, Massey A, Newman TA, et al. Cerebral amyloid angiopathy: Amyloid beta accumulates in putative interstitial fluid drainage pathways in Alzheimer's disease. Am J Pathol 1998;153:725–33
27. McGeer PL, McGeer EG. The inflammatory response system of brain: Implications for therapy of Alzheimer and other neurodegenerative diseases. Brain Res Brain Res Rev 1995;21:195–218
28. Meda L, Cassatella MA, Szendrei GI, et al. Activation of microglial cells by beta-amyloid protein and interferon-gamma. Nature 1995;374:647–50
29. Weldon DT, Rogers SD, Ghilardi JR, et al. Fibrillar beta-amyloid induces microglial phagocytosis, expression of inducible nitric oxide synthase, and loss of a select population of neurons in the rat CNS in vivo. J Neurosci 1998;18:2161–73
30. Wisniewski HM, Barcikowska M, Kida E. Phagocytosis of beta/A4 amyloid fibrils of the neuritic neocortical plaques. Acta Neuropathol (Berl) 1991;81:588–90
31. Rogers J, Strohmeyer R, Kovelowski CJ, Li R. Microglia and inflammatory mechanisms in the clearance of amyloid beta peptide. Glia 2002;40:260–69
32. Herber DL, Roth LM, Wilson D, et al. Time-dependent reduction in Abeta levels after intracranial LPS administration in APP transgenic mice. Exp Neurol 2004;190:245–53
33. Akiyama H, McGeer PL. Specificity of mechanisms for plaque removal after A beta immunotherapy for Alzheimer disease. Nat Med 2004;10:117– 18; [author reply 8–9]
34. Sawada M, Imamura K, Nagatsu T. Role of cytokines in inflammatory process in Parkinson's disease. J Neural Transm Suppl 2006;(70):373–81
35. Schwartz M, Butovsky O, Bruck W, Hanisch UK. Microglial phenotype: Is the commitment reversible? Trends Neurosci 2006;29:68–74
36. Schwartz M. Macrophages and microglia in central nervous system injury: Are they helpful or harmful? J Cereb Blood Flow Metab 2003;23:385–94
37. Song YK, Liu F, Chu S, Liu D. Characterization of cationic liposome–mediated gene transfer in vivo by intravenous administration. Hum Gene Ther 1997;8:1585–94

Nonviral Aβ DNA vaccine therapy against Alzheimer's disease: Long-term effects and safety

Yoshio Okura*, Akira Miyakoshi*, Kuniko Kohyama*, Il-Kwon Park*, Matthias Staufenbiel†, and Yoh Matsumoto*‡

*Department of Molecular Neuropathology, Tokyo Metropolitan Institute for Neuroscience, Musashidai 2-6, Fuchu, Tokyo 183-8526, Japan; and †Neuroscience Research, Novartis Institutes of Biomedical Research, CH-4002 Basel, Switzerland

Edited by Hugh O. McDevitt, Stanford University School of Medicine, Stanford, CA, and approved May 10, 2006 (received for review February 6, 2006)

It was recently demonstrated that amyloid β (Aβ) peptide vaccination was effective in reducing the Aβ burden in Alzheimer model mice. However, the clinical trial was halted because of the development of meningoencephalitis in some patients. To overcome this problem, anti-Aβ antibody therapy and other types of vaccination are now in trial. In this study, we have developed safe and effective nonviral Aβ DNA vaccines against Alzheimer's disease. We administered these vaccines to model (APP23) mice and evaluated Aβ burden reduction. Prophylactic treatments started before Aβ deposition reduced Aβ burden to 15.5% and 38.5% of that found in untreated mice at 7 and 18 months of age, respectively. Therapeutic treatment started after Aβ deposition reduced Aβ burden to≈50% at the age of 18 months. Importantly, this therapy induced neither neuroinflammation nor T cell responses to Aβ peptide in both APP23 and wild-type B6 mice, even after long-term vaccination. Although it is reported that other anti-Aβ therapies have pharmacological and/or technical difficulties, nonviral DNA vaccines are highly secure and easily controllable and are promising for the treatment of Alzheimer's disease.

amyloid β-peptide | DNA vaccination

Alzheimer's disease is a chronic neurodegenerative disorder that is the most common cause of progressive impairment of memory and cognitive function in aged humans. The etiology of the disease is thought to be the result of an imbalance between amyloid β (Aβ) production and clearance (amyloid cascade hypothesis) (1, 2). On the basis of this hypothesis, Schenk *et al.* (3) developed an Aβ-peptide vaccine, immunized amyloid precursor protein (APP)-transgenic mice with the peptide in complete Freund's adjuvant (CFA), and demonstrated a marked amyloid reduction in the brain. Repetitive intranasal administration of Aβ-peptide and adjuvant (4) and the passive transfer of anti-Aβ antibodies were also effective in reducing amyloid deposits (5). Moreover, vaccinated mice showed an improvement in memory loss (6, 7). Thus, Aβ peptide vaccine therapy has been shown to be effective in animal models, and human clinical trials were started with Betabloc (AN-1792), composed of synthetic Aβ1-42 and QS21 as an adjuvant (8). However, the phase II clinical trial was halted because of the development of acute meningoencephalitis that appeared in 18 (6%) of 298 vaccinated patients (9). Importantly, it was later demonstrated by autopsy that there was a significant reduction of amyloid deposition and disappearance of degenerative axons in a treated patient (10). At the same time, T cell-dominant meningeal encephalitis was present in the cerebral cortex. These findings suggest that the vaccine therapy is a promising strategy for human Alzheimer's disease if excessive immune reactions are minimized to avoid unwanted neuroinflammation.

Recently, it was reported that naked plasmid DNAs encoding proteins are taken into cells and produce the proteins in a small amount for a relatively long period when injected into the muscle or skin (11). Then, the proteins that are released in the extracellular space induce antibodies against the proteins (12, 13). Thus, gentle and quiet immune reactions could be obtained by DNA vaccine administration. In our and other's laboratories, immune therapies with DNA vaccines have been examined in autoimmune disease models (14–17) and have been found to be effective in preventing the diseases without the use of adjuvants. Here, we developed nonviral Aβ DNA vaccines and were able to reduce the amyloid burden in the cerebral cortex and hippocampus of Alzheimer's disease model (APP23) mice by vaccination. Importantly, the side effects, such as T cell proliferation and neuroinflammation, were absent even after long-term administration of the vaccines in both APP23 and wild-type B6 mice.

Results

Preparation and Characterization of Nonviral Aβ DNA Vaccines. We prepared three types of nonviral Aβ DNA vaccines using a mammalian expression vector, pTarget. The sequence of Aβ1-42 and additional sequences were inserted in the plasmid, as shown in Fig. 1*A*. The first one contains only the Aβ1-42 sequence with the Kozak sequence at the 5′ end (referred to as K-Aβ vaccine) (Fig. 1*A1*). To the second, the Igκ signal sequence of mouse Ig was added to improve the secretion ability (IgL-Aβ vaccine) (Fig. 1*A2*), and the third possesses the Fc portion of human Ig at the 3′ end to maintain stability (Aβ-Fc vaccine) (Fig. 1*A3*). Before *in vivo* administration, these DNA vaccines were transfected to HEK295T cells, and the secretion of Aβ1-42 peptide into the culture supernatant was assayed with Western blotting (Fig. 1*B*). The production of intracellular Aβ1-42 peptide was confirmed in all three vaccines by ELISA (data not shown). It was clearly demonstrated that the supernatants of cultured cells that had been transfected with IgL-Aβ and Aβ-Fc vaccines contained translated proteins (4.5 and 35 kDa, respectively), whereas K-Aβ-transfected cells did not secrete the peptide into the extracellular space. These findings indicate that the addition of the leader sequence is important for transportation of the protein to the extracellular space as reported in ref. 18 and that this event is critical for the effects of DNA vaccines (see below).

Reduction of Amyloid Burden by Aβ DNA Vaccination. We used two types of regimens to examine the effect of Aβ DNA vaccination, i.e., prophylactic and therapeutic. For the prophylactic protocol, vaccine administration was started at 3–4 months of age, before the appearance of amyloid deposition. APP23 mice received 6 weekly and subsequent biweekly injections of the vaccines and were examined at 7, 9, 12, 15, and 18 months of age (Fig. 1*C1*). The paraffin-embedded sections of the brain were stained immunohistochemically with 6F/3D against Aβ8-17, and the area of amyloid depositions was quantitated as the total sum of the pixels with NIH IMAGE software.

Conflict of interest statement: M.S. is employed by and a shareholder of Novartis Institutes of Biomedical Research.

This paper was submitted directly (Track II) to the PNAS office.

Abbreviations: Aβ, amyloid β; Aβ-Fc, IgL-Aβ-pTarget, the Fc portion of immunoglobulin; APP, amyloid precursor protein; CFA, complete Freund's adjuvant; IgL-Aβ, immunoglobulin leader sequence-Aβ-pTarget; K-Aβ, Kozak-Aβ-pTarget; Th, T helper.

‡To whom correspondence should be addressed. E-mail: matyoh@tmin.ac.jp.

Fig. 1. Construction of DNA vaccines (*A*), *in vitro* characterization (*B*) and the treatment protocol (*C*). (*A*) Three DNA vaccines were produced by using a mammalian expression vector. DNA encoding the Aβ1-42 sequence was inserted in XhoI/KpnI site of the plasmid (K-Aβ vaccine) (*A1*). In the second vaccine, the signal sequence of mouse Igκ is added to the 5′ end to improve the secretive efficiency (IgL-Aβ vaccine) (*A2*). The third vaccine possesses the Fc portion of human immunoglobulins to improve the stability of the secreted protein (Aβ-Fc vaccine) (*A3*). (*B*) Western blot analysis revealed that translated Aβ proteins were detected in supernatants of cultured cells transfected with IgL-Aβ and Aβ-Fc vaccines. (*C*) The protocol of vaccine treatment. To examine the prophylactic effect of DNA vaccines, the vaccines were administrated to APP23 mice starting from 3–4 months of age, before the appearance of amyloid depositions. The mixture of one of the vaccines (100 μg) and bupivacaine (0.25 mg) was injected intramuscularly on a weekly basis for the first 6 weeks. Then, the vaccine without bupivacaine was injected every 2 weeks thereafter. Mice were sampled at 7, 9, 12, 15, and 18 months of age (*C1*). For therapeutic treatment, the vaccines were administered to APP23 mice starting from 12 months of age, after the appearance of amyloid plaques. Samplings were performed at 15 and 18 months of age (*C2*). m, months of age.

In the first series of the prophylactic treatment, mice were analyzed at 7, 9, and 12 months of age (Table 1, Exp. 1). At 7 months of age, granular amyloid depositions were recognized in the frontal cortex in the control groups (empty-vector-administered and untreated mice) (Fig. 2*B*). At this stage, Aβ plaques were not detected in the hippocampus (data not shown). In sharp contrast, cortical Aβ depositions in mice treated with Aβ-Fc (Fig. 2*A*), IgL-Aβ, and Aβ (data not shown) vaccines were significantly reduced ($P < 0.01$). The Aβ burden was reduced to ≈15–30% of the untreated groups (Fig. 2*E*). At 12 months of age, amyloid depositions in untreated mice were increased, and some of them became large (>50 μg) in the frontal cortices of the untreated mice (Fig. 4*C*, which is published as supporting information on the PNAS web site). Cortical

Table 1. Summary of experimental data on nonviral Aβ DNA vaccine therapy against Alzheimer model mice

Exp.	Group	Strain	No. of animals	Start of Tx, mo	Sampling, mo	Duration of Tx, mo	Protocol: Regimen	Protocol: Weekly	Protocol: Biweekly	Protocol: Monthly	% Aβ burden (cortex): Fc	IgL	K-Aβ	Emp	No Tx	% Aβ burden (hippocampus): Fc	IgL	K-Aβ	Emp	No Tx	Inflammation: CD5	Mac3
1	1	Tg	15	4	7	3	Prophylactic	×6	×3		15.5	18.2	31.4	93.1	100	N.T.	N.T.	N.T.	N.T.	N.T.	Neg	Neg
	2	Tg	32	4	9	5	Prophylactic	×6	×8		12.7	13.3	28.1	103	100	N.T.	N.T.	N.T.	N.T.	N.T.	Neg	Neg
	3	Tg	17	4	12	8	Prophylactic	×6	×12		33.7	28.6	51.3	103	100	22	26	65.3	114	100	Neg	Neg
2	1	Tg	20	3	15	12	Prophylactic	×6	×24		30.6	37.2	N.T.	91.2	100	32.5	38.4	N.T.	96	100	Neg	Neg
	2	Tg	16	3	18	15	Prophylactic	×6	×29		38.5	46.2	N.T.	91.3	100	36.4	44.8	N.T.	99.5	100	Neg	Neg
3	1	Tg	23	12	15	3	Therapeutic	×6	×4		42.4	41.6	N.T.	98.1	100	40.3	43.5	N.T.	100	100	Neg	Neg
	2	Tg	19	12	18	6	Therapeutic	×6	×10		47	49.9	N.T.	96.7	100	38	46	N.T.	86.6	100	Neg	Neg
4	1	Tg	18	7	15	8	Therapeutic			×9	67.6	81.7	N.T.	90.6	100	69.4	73.9	N.T.	95.6	100	Neg	Neg
	2	Tg	16	7	18	11	Therapeutic			×12	79.6	88.1	N.T.	91.7	100	74.8	75.6	N.T.	92	100	Neg	Neg
5	1	B6	25	4	7	3	–	×6	×4		N.T.	N.T.	N.T.	N.T.	N.T.	N.T.	N.T.	N.T.	N.T.	N.T.	Neg	Neg
	2	B6	25	4	9	5	–	×6	×9		N.T.	N.T.	N.T.	N.T.	N.T.	N.T.	N.T.	N.T.	N.T.	N.T.	Neg	Neg
	3	B6	24	4	12	8	–	×6	×14		N.T.	N.T.	N.T.	N.T.	N.T.	N.T.	N.T.	N.T.	N.T.	N.T.	Neg	Neg

The vaccines were administered for the indicated duration to a large number of mice (176 APP23 and 74 B6 mice). In Exp. 1, the mice were divided into five groups as follows: Aβ-Fc vaccine administration, IgL-Aβ vaccine administration, K-Aβ vaccine administration, empty-vector administration, and no treatment. In Exps. 2–5, the K-Aβ vaccine administration group was excluded from the analysis because of its lower efficacy than other two vaccines. Each group consisted of 4–6 mice. Prophylactic effects were examined in Exps. 1 and 2. Therapeutic effects were examined in Exps. 3 and 4. All APP23 mice were analyzed immunohistochemically with mAb (6F/3D) against Aβ7-18. Then, the reduction of amyloid plaque was quantified, as shown in *Materials and Methods*. In Exp. 5, DNA vaccines were administered to B6 mice to know whether the vaccines induce neuroinflammation. Tissues from three mice in each group were immunohistochemically stained with mAbs against CD5 and Mac-3. Neg, negative finding, i.e., no neuroinflammation; N.T., not tested; Exp., experiment; Tx, treatment; Tg, transgenic; Emp, empty vector.

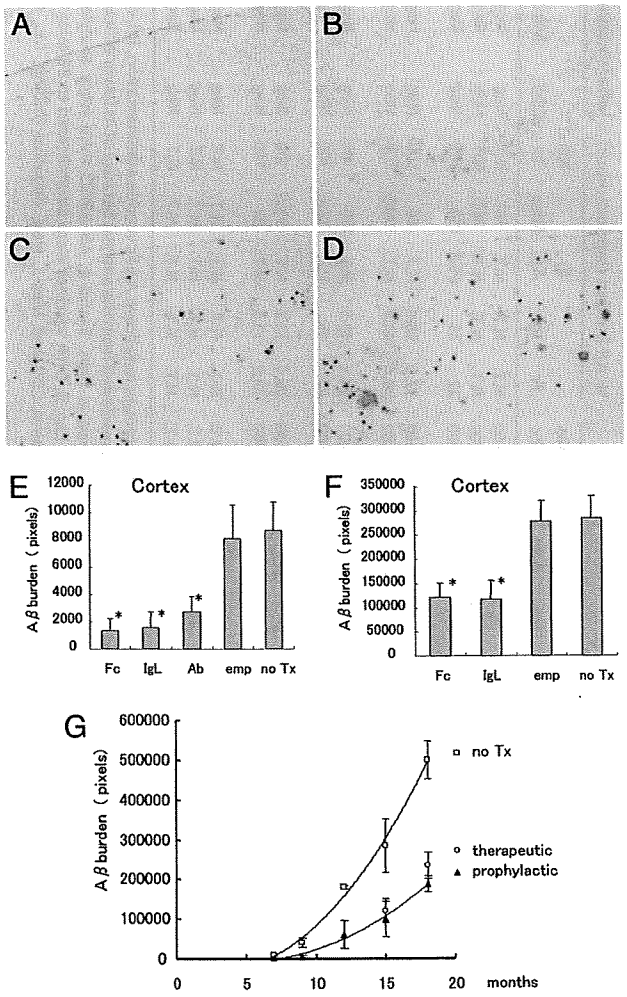

Fig. 2. Reduction of Aβ burden in APP23 mice after DNA vaccination. (*A*) In mice vaccinated with Aβ-Fc vaccine, amyloid plaques in the frontal cortex were reduced after 3 months of prophylactic treatment. (*B*) Immunohistochemical examinations revealed that granular amyloid depositions were detected in the frontal cortices of untreated mice at 7 months of age. (*C*) Amyloid plaques were reduced in mice treated with Aβ-IgL vaccine. (*D*) At 15 months of age amyloid plaques of variable size were detected in the frontal cortices of untreated mice. (*E*) Quantitative analysis demonstrated that the cortical Aβ burden at 7 months was significantly decreased ($P < 0.01$) after the prophylactic treatment with Aβ-Fc (15.5% of untreated controls), IgL-Aβ (18.2%), and Aβ vaccine (31.4%) compared with those found in untreated and empty-vector-vaccinated mice. (*F*) Therapeutic treatment with Aβ-Fc and IgL-Aβ vaccines significantly reduced ($P < 0.01$) cortical Aβ burden at 15 months. The overall quantitative analysis is depicted in *G*. The amyloid deposition was first detected in untreated mice at 7 months of age and rapidly increased after 15 months of age (open squares). Prophylactic administration of Fc-Aβ vaccine prevented the Aβ deposition to 10–30% of that in untreated animals before 12 months of age and to 40–50% after 15 months (filled triangles). The effects of therapeutic administration were almost the same as those of prophylactic administration (open circles). Tx, treatment; emp, empty vector. Original magnification, ×62 (*A* and *B*); ×24 (*C* and *D*).

Aβ depositions were significantly reduced ($P < 0.01$) to ≈30–50% of the untreated group (Fig. 4*D*) after Aβ-Fc (Fig. 4*A*) and IgL-Aβ (Fig. 4*B*) vaccine treatment. Aβ depositions in the hippocampus were also decreased equally ($P < 0.01$) (Table 1, Exp. 1, Group 3). It was shown that the suppressive effect of Aβ-Fc vaccine was almost equal to IgL-Aβ vaccine. However, K-Aβ vaccine was less effective than the former two (Figs. 2*E* and 4*D*) and was not used in subsequent experiments. The second part of the prophylactic treatment analyzed the mice at 15 and 18 months of age (Table 1, Exp. 2). At these time points, the plaques in untreated groups had rapidly increased. Untreated APP23 mice showed an age-dependent increase of amyloid plaques in the cerebral cortex (Fig. 2*G*, open squares) and hippocampus (data not shown). The prophylactic protocol, using Aβ-Fc vaccine, revealed that the final reduction rate of Aβ burden in the cerebral cortex at 18 months of age was ≈38.5% of untreated groups (Table 1, Exp. 2 and Fig. 2*G*, closed triangles). These results demonstrated that two of the three vaccines produced in this study were effective in prophylactic treatment.

When considering the clinical applications, it is critical to know the effects of the vaccines in therapeutic application. For this purpose, the vaccination was started at 12 months of age, 6 months after the start of Aβ deposition, and the brains were examined at 15 (Fig. 2) and 18 (Fig. 5, which is published as supporting information on the PNAS web site) months of age. In therapeutic treatment, amyloid plaques in the cortex were significantly decreased ($P < 0.01$) (Fig. 2*F*) by Aβ-Fc and IgL-Aβ vaccination (Fig. 2*D*) compared with the controls (Fig. 2*C*). Aβ depositions in the hippocampus were also decreased ($P < 0.01$) (Table 1, Exp. 3). Although the therapeutic protocol (Fig. 2*G*, open circles) seemed to be less effective than the prophylactic one (Fig. 2*G* closed triangles), the difference was not significant. It should be noted that APP23 mice treated with the therapeutic protocol received DNA vaccines for only 3 and 6 months, respectively (Table 1, Exp. 3). Thus, Aβ DNA vaccines had sufficient effects, even if the vaccines were administrated after amyloid depositions appeared.

Recently, it was reported that the intracellular Aβ deposition in cortical pyramidal neurons is the first neurodegenerative event in Alzheimer's disease development (19). Therefore, we counted the number of neurons containing intracellular Aβ depositions in the cortices of Aβ-Fc-vaccine-administered and control mice. Aβ-deposited neurons were significantly decreased with both the prophylactic (50.2% of untreated control, $P < 0.01$) and therapeutic (59.54%, $P < 0.05$) treatments at 15 months of age (Fig. 6, which is published as supporting information on the PNAS web site).

Change in the Serum Aβ Antibody Titer After Vaccine Administration. The titers of serum anti-Aβ antibodies after the prophylactic treatment (Table 1, Exps. 1 and 2) were determined by ELISA. The levels of anti-Aβ antibodies were significantly increased (**, $P < 0.01$; *, $P < 0.05$) 2- to 4-fold compared with the untreated and empty-vector-vaccinated mice (Fig. 3*A*). The titers showed an age-dependent increase in both treated and untreated mice, because the antibody production was induced in untreated APP23 mice by high levels of Aβ in the sera of aged mice. In contrast, the anti-Aβ antibodies in the sera of wild-type B6 mice were below the detection limit (data not shown). We also analyzed the relationships between the amounts of amyloid depositions and anti-Aβ titers (Fig. 3*B*). The amounts of amyloid depositions were significantly smaller in mice with high antibody titers. A significant correlation between the antibody titer and the reduction of Aβ burden was observed at 7 months ($r = -0.642$) (Fig. 3*B*, 7 months) and 9 months ($r = -0.38965$) (Fig. 3*B*, 9 months) of age by the CORREL function. The difference became less clear at a later stage (Fig. 3*B*, 12 months).

T Cell-Proliferation Assay After Vaccine Administration. To determine whether DNA vaccination induces the T cell activation and proliferation that are key steps for the development of neuroinflammation, APP23 and B6 mice were injected with DNA vaccines. A group of mice were also immunized with Aβ peptide/CFA. Three weeks after the first injection, lymphocytes were isolated and cultured with Aβ peptide (0–10 μM) for 3

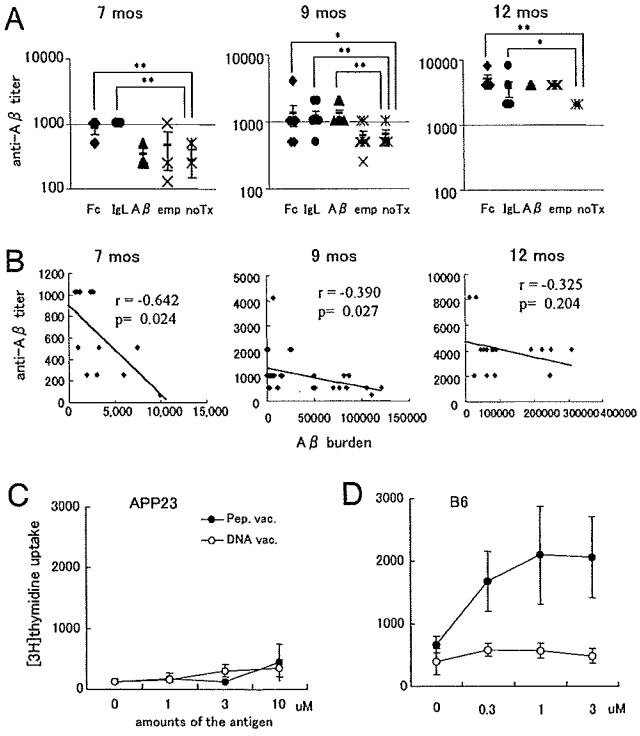

Fig. 3. B and T cell responses of mice treated with Aβ DNA vaccines. (*A* and *B*) Titration of anti-Aβ antibodies in vaccinated APP23 mice. The anti-Aβ antibody titer in treated mice was significantly increased (**, $P < 0.01$; *, $P < 0.05$) ≈2- to 4-fold compared with the untreated group. The titer levels were increased in untreated APP23 as well as treated mice at the same age period (*A*). There was significant correlation between the serum anti-Aβ antibody titer and the reduction of amyloid depositions at 7 months of age (CORREL function $r = -0.642$, $t0 = 2.648 > t10 = 2.228$) (*B*). At 9 months of age, a significant correlation was present, but the difference was less marked compared with that at 7 months ($r = -0.38965$, $t0 = 3.10 > t22 = 2.086$). A significant difference was not noted at 12 months of age ($r = -0.325$, $t0 = 1.3309 < t17 = 2.110$). (*C* and *D*) T cell responses in APP23 (*C*) and B6 (*D*) mice after immunization with Aβ peptide/CFA or DNA vaccination. Lymphocytes isolated from two strains were incubated with Aβ peptide (0–10 μM) for 3 days. Incorporation of [^{3}H]thymidine was measured by liquid scintillation spectrometry. In APP23 mice, neither T cells from peptide-immunized mice nor those from DNA-vaccinated mice were activated in the presence of Aβ1-42 (*C*). In contrast, Aβ peptide immunization, but not DNA vaccination, induced a significant T cell response in B6 mice (*D*). All of the data are the mean values ± SD, and the representative results from three different experiments are shown. Tx, treatment; emp, empty vector.

days. Incorporation of [^{3}H]thymidine was measured by using liquid scintillation spectrometry. T cells from APP23 mice did not react with Aβ peptide after both Aβ DNA vaccine and Aβ peptide administration (Fig. 3*C*). In sharp contrast, T cells from B6 mice responded significantly to Aβ peptide after immunization with Aβ peptide, but not after Aβ DNA vaccination (Fig. 3*D*). Notably, Aβ DNA vaccination did not induce T cell proliferation in either APP or B6 mice after three injections (Fig. 3*C*) and 5-month treatment (data not shown). These findings suggest that T helper (Th)1 cells in APP23 mice are in an immunologically tolerant state against Aβ1-42, probably because of long-term exposure to a high level of Aβ1-42.

Pathological Examination of the Brains of Vaccinated Mice. The presence or absence of neuroinflammation in the brain was examined immunohistochemically after the long-term administration of DNA vaccines. Because the T cell assay demonstrated the significant differences between APP23 and B6 mice, pathological examinations were performed in both strains. Brain sections were stained with anti-CD5 mAb against T cells and with Mac-3 against macrophages. In the thymus (Fig. 7*A*, which is published as supporting information on the PNAS web site) and spleen (Fig. 7*B*), a large number of lymphocytes and macrophages were stained positively. In sharp contrast, inflammatory foci in the brain parenchyma and meninges were not detected in either APP23 (Fig. 7 *C* and *D*) or B6 (Fig. 7 *E* and *F*) mice.

Discussion

In this study, we developed nonviral Aβ DNA vaccines against Alzheimer's disease and demonstrated satisfactory effects in the Aβ reduction in model mice. With the prophylactic and therapeutic protocols, treatment with both IgL-Aβ and Aβ-Fc reduced Aβ burden in the cerebral cortex to ≈40–50% of the untreated controls, although the latter was slightly more effective than the former. It should be noted that mice killed at 18 months of age received DNA vaccines for only the last 6 months. These findings suggest that relatively short-term vaccination is sufficient for the reduction of Aβ burden. Because it was demonstrated in the other experimental setting that 50% reduction of Aβ burden resulted in full recovery of the cognitive disturbance (6), the suppressive effects of DNA vaccines demonstrated in this study is satisfactory. Furthermore, it was reported that Aβ immunotherapy reduces not only extracellular Aβ plaques but also intracellular Aβ accumulation and, most notably, leads to the clearance of early tau pathology by using the triple-transgenic model of Alzheimer's disease (20–22). Taken together, the outcome of DNA vaccine therapy is promising when applied to human Alzheimer's disease.

The elevation of anti-Aβ antibodies was also detected after DNA vaccination. However, the antibody elevation was mild to moderate (≈2- to 4-fold) compared with that found in mice that had received Aβ peptide (10,000-fold) (3). The adjuvant in peptide vaccines (23) may activate Th1 type T cells (10), which induce the rapid increase of antibody titers as a result. As demonstrated in this study, DNA vaccination was able to be performed without adjuvants, resulting in the absence of obvious T cell proliferation in both APP23 and B6 mice (Fig. 7) and did not cause neuroinflammation, even after long-term DNA vaccination (Fig. 7, which is published as supporting information on the PNAS web site). Importantly, mild elevation of the antibody titers induced by DNA vaccines could reduce amyloid deposits, probably because DNA vaccination constantly induces the antibody production at a low titer for a long period. Thus, the maintenance of high anti-Aβ antibody titer levels is not necessary for effective treatment with DNA vaccines.

To minimize excessive immune reaction in mice and patients, we should recognize the difference in immunological reactions against Aβ between the Alzheimer model and wild-type mice. As clearly demonstrated here, there was no Th1 cell response to Aβ peptide in APP23 mice after Aβ peptide/CFA injection, whereas, in B6 mice, the same immunization protocol induced a significant T cell response against Aβ peptide (Fig. 3*D*). These findings strongly suggest that autoreactive Th1 cells in model mice are in a state of immune tolerance because of a high Aβ expression from an early stage of life. In contrast, Th2 cells helping the antibody production seem to be working, as evidenced by the fact that vaccinated animals possessed elevated levels of anti-Aβ antibodies. Similar findings were reported by Qu *et al.* (24), with gene-gun administration of Aβ plasmid DNA. Monsonego *et al.* (25) also reported that the immune responses of T and B cells of model mice are low compared with those of wild-type mice. In contrast, a significant T cell reactivity to Aβ peptide was detected in patients with Alzheimer's disease (23). Thus, strong immune induction is dangerous for patients with Alzheimer's disease.

The CpG motif, which exists in plasmid DNAs, is reported to induce Th1-type immunity and up-regulates IFN-γ production under certain circumstances (26–28). However, this phenomenon is observed only when a relatively high dose of CpG oligonucleotides is used (29). In contrast, empty vectors containing the CpG motif ameliorated the clinical and histological severity of the autoimmune encephalomyelitis that is thought to be a Th1-mediated disease, as shown in previous studies by us (30) and others (31, 32).

Recently, Aβ DNA vaccines were developed by using virus vectors (33, 34). Although, these vaccines effectively decreased Aβ depositions in the brains of model mice, the possibility of viral replication could not be completely excluded. The plasmid vector is safe and has no possibility of viral infection and transformation because it exists as an episome without being built into the chromosome in eukaryotic cells (12, 13). Another important factor is related to technology. When DNA vaccines are in clinical use, large amounts of vaccines are necessary for treatment of a large number of patients who would be treated for a long period. Nonviral DNA vaccines have an advantage because they can be mass-produced with a high purity at a low price.

In summary, we demonstrated that nonviral Aβ DNA vaccines are highly effective and safe in reducing the Aβ burden in model mice and, thus, are promising as a vaccine therapy against human Alzheimer's disease.

Materials and Methods

Animals. The APP23 transgenic mice used in this study express human APP751 cDNA with Swedish double mutation under the control of the neuron-specific mouse Thy-1 promoter (35, 36). The Thy-1 expression cassette lacks intron 3, which contains the elements required for expression in the thymus. RT-PCR and Western blot analysis of APP23 mice have confirmed the lack of detectable expression of the transgene in the thymus and spleen (D. Abramowski, C. Sturchler-Pierrat, and M.S., unpublished data). This finding is in agreement with a report by Moechars *et al.* (37), who used the same expression cassette and also found that the exogenous transgene with this promoter sequence is expressed only in the brain but not in the thymus. APP23 mice were initially established on a B6D2 background and have been continuously backcrossed to C57BL/6J (B6). In APP23 mice, amyloid depositions appear from 6 months of age, predominantly in the neocortex and hippocampus. Aβ plaques have most of the characteristics of human Alzheimer's disease plaques, including fibrillary Aβ cores, and are surrounded by dystrophic neuritis and activated glial cells. Region-specific amyloid-associated neurodegeneration, including neuron loss, synapse deficits, and cholinergic alterations, are present in these mice (38). Wild-type B6 mice were purchased from Charles River Breeding Laboratories (Kanagawa, Japan). All animal experiments were approved by the institute committee and performed in accordance with institutional guidelines.

The Development of DNA Vaccine. We prepared three Aβ DNA vaccines using a pTarget mammalian expression system (Promega, Tokyo) (Fig. 1*A*). The DNA fragment, encoding Aβ1-42, was made to anneal two oligonucleotides covering the entire Aβ1-42 sequence. The Kozak sequence was inserted at the 5′ end of the Aβ1-42 sequence (referred to as K-Aβ vaccine). In the second vaccine, the signal sequence of mouse Igκ was added to the 5′ end of the Aβ1-42 sequence to improve the secretory efficiency of Aβ peptide (IgL-Aβ vaccine). The third vaccine was made by adding the Fc portion of human immunoglobulins to the 3′ end of the Aβ1-42 sequence to stabilize the secreted protein (Aβ-Fc vaccine). To prevent unwanted disulfide bonds, three cystines in the sequence were substituted with serine.

Transfection of DNA Vaccines and Western Blot Analysis. Three DNA vaccines were transfected to HEK293T cells and the amounts of produced Aβ peptide were measured by using ELISA. HEK293T cells in 60–70% confluence were prepared on 6-well plates (Costar, Cambridge, MA). The cells were first cultured in serum-free RPMI medium 1640 for 2 h with one of three DNA vaccines (K-Aβ, IgL-Aβ, or Aβ-Fc) and Lipofectamine PLUS reagent (Invitrogen). Then, the cells were cultured overnight in RPMI medium 1640 supplemented with 5% FBS for cellular stabilization and growth. For the Western blot analysis, the cells were again cultured in serum-free medium for an additional 8 h to remove unnecessary proteins.

Culture supernatants and cell pellets were harvested and run on NuPAGE 12% Bis-Tris gel (Invitrogen) and transferred to the PVDF membrane (Immobilon-P; Millipore). After blocking with 10% nonfat milk, the blots were incubated with 6E10 (anti-human Aβ1–17 antibody, 1:100; Abcam, Cambridge, U.K.) at 4°C for 1 h, followed by incubation with biotin-conjugated anti-mouse IgG (1:1,000; Vector Laboratories) for 1 h and with ABC-HRP (VectorLaboratories) for 1 h. The blots were developed by enhanced chemiluminescence reagents (Immunostar kit; Wako Biochemicals) according to the manufacturer's instructions.

Administration of the Vaccines. DNA vaccines (100 μg) and bupivacaine (0.25 mg) in 100 μl was administered i.m. on a weekly basis for 6 weeks (39). The vaccines without bupivacaine were injected biweekly thereafter. To examine the prophylactic effect, vaccination was started at 3–4 months of age, before amyloid plaque appearance. The therapeutic treatment was started at 12 months of age, after amyloid plaque appearance.

Immunohistochemistry. Mice were killed under deep anesthesia, and the brains were removed and immersion-fixed in 4% paraformaldehyde. Paraffin-embedded sections (6 μm) were stained immunohistochemically with mAb (6F/3D) against Aβ8–17 (DAKO), anti-CD5 mAb against T lymphocytes (BD Biosciences Pharmingen) and Mac-3 against mononuclear phagocytes (BD Biosciences Pharmingen). For 6F/3D staining, the sections were pretreated in formic acid for 3 min. The sections were then incubated in the primary antibody at a 1:200 dilution. After washing, the sections were incubated with biotinylated horse anti-mouse IgG (Vector Laboratories), followed by a horseradish peroxidase (HRP)-labeled Vectastain Elite ABC kit (Vector Laboratories). HRP-binding sites were detected in 0.005% diaminobenzidine and 0.01% hydrogen peroxide. CD5 (1:25) and Mac-3 (1:25) stainings were performed similarly, with overnight incubation of the primary antibodies.

Quantitative Analysis of Aβ Burden. Aβ burdens were quantitated in the cerebral cortex and hippocampus, according to the method described in ref. 40. All of the procedures were performed by an individual blind to the experimental condition of the study. The images under an Olympus Vanox microscope were captured with a 3 charge-coupled device Olympus digital camera. The amyloid load was measured in 10 fields from the cingulated to retrosplenial cortex in the left hemispheres of the mice (600 × 400 μm each), chosen randomly. Analysis in the hippocampus was performed on the entire hippocampus in a similar manner. Aβ depositions that occupied the field were expressed as pixels by using the NIH IMAGE software.

ELISA. Microtiter plates were coated with 2 μg/ml human Aβ1-40 (Peptide Institute, Osaka) in 0.1 M sodium carbonate buffer (pH 9.5) at 4°C overnight. After washing three times, plates were incubated for 2 h with serial dilutions of plasma samples in PBS in 12 rows of wells starting with 4-fold-diluted plasma (the greatest dilution tested was 1:213). The plates were washed and

incubated with a 1,000-fold dilution of biotinylated anti-mouse IgG (Vector Laboratories), followed by incubation with 2-fold dilutions of Vectastain ABC-kit solution (Vector Laboratories). Bound antibodies were detected by using SIGMA FAST (Sigma-Aldrich), and the absorbance at 450 nm was read on an automated plate reader (Model 550; Bio-Rad). The antibody titer was defined as the reciprocal of the greatest dilution of plasma that gives half-maximal binding to Aβ, which was determined by dividing the highest OD_{450} value in the dilution range of each sample by 2.

T Cell-Proliferation Assay. The proliferative responses of draining lymph node cells were assayed in microtiter plates (Costar, Cambridge, MA) by the uptake of [^{3}H]thymidine. Aβ1-42 peptide (50 μg) emulsified with CFA (twice) and Fc-Aβ vaccine (three times) was injected into APP23 mice or B6 mice, and then the drainage lymph nodes were taken 3 weeks after the first injection. Lymph node cells (2×10^5 cells per well) were cultured with 0.3–10 μM Aβ1-42 peptide for 3 days and subsequently pulsed for 18 h with 0.5 μCi (1 Ci = 37 GBq) of [^{3}H]thymidine (Amersham Pharmacia Biotech). Incorporation of [^{3}H]thymidine was measured by liquid scintillation spectrometry.

Statistical Analysis. Student's t test or Mann–Whitney's U test was used for the statistical analysis. Correlations between the antibody titer and the reduction of Aβ burden was estimated by the CORREL function.

We thank Y. Kawazoe for technical assistance. This study was supported, in part, by Grants-in-Aid from the Ministry of Education, Japan, and a grant from Novartis Institutes of Biomedical Research.

1. Hardy, J. & Selkoe, D. J. (2002) *Science* **297,** 353–356.
2. Selkoe, D. J. & Schenk, D. (2003) *Annu. Rev. Pharmacol. Toxicol.* **43,** 545–584.
3. Schenk, D., Barbour, R., Dunn, W., Gordon, G., Grajeda, H., Guido, T., Hu, K., Huang, J., Johnson-Wood, K., Khan, K., *et al.* (1999) *Nature* **400,** 173–177.
4. Weiner, H. L., Lemere, C. A., Maron, R., Spooner, E. T., Grenfell, T. J., Mori, C., Issazadeh, S., Hancock, W. W. & Selkoe, D. J. (2000) *Ann. Neurol.* **48,** 567–579.
5. Bard, F., Cannon, C., Barbour, R., Burke, R. L., Games, D., Grajeda, H., Guido, T., Hu, K., Huang, J., Johnson-Wood, K., *et al.* (2000) *Nat. Med.* **6,** 916–919.
6. Janus, C., Pearson, J., McLaurin, J., Mathews, P. M., Jiang, Y., Schmidt, S. D., Chishti, M. A., Horne, P., Heslin, D., French, J., *et al.* (2000) *Nature* **408,** 979–982.
7. Morgan, D., Diamond, D. M., Gottschall, P. E., Ugen, K. E., Dickey, C., Hardy, J., Duff, K., Jantzen, P., DiCarlo, G., Wilcock, D., *et al.* (2000) *Nature* **408,** 982–985.
8. Hock, C., Konietzko, U., Papassotiropoulos, A., Wollmer, A., Streffer, J., von Rotz, R. C., Davey, G., Moritz, E. & Nitsch, R. M. (2002) *Nat. Med.* **8,** 1270–1275.
9. Orgogozo, J. M., Gilman, S., Dartigues, J. F., Laurent, B., Puel, M., Kirby, L. C., Jouanny, P., Dubois, B., Eisner, L., Flitman, S., *et al.* (2003) *Neurology* **61,** 46–54.
10. Nicoll, J. A., Wilkinson, D., Holmes, C., Steart, P., Markham, H. & Weller, R. O. (2003) *Nat. Med.* **9,** 448–452.
11. Wolff, J. A., Malone, R. W., Williams, P., Chong, W., Acsadi, G., Jani, A. & Felgner, P. L. (1990) *Science* **247,** 1465–1468.
12. Nishikawa, M. & Huang, L. (2001) *Hum. Gene. Ther.* **12,** 861–870.
13. Nishikawa, M. & Hashida, M. (2002) *Biol. Pharm. Bull.* **25,** 275–283.
14. Lobell, A., Weissert, R., Storch, M. K., Svanholm, C., de Graaf, K. L., Lassmann, H., Andersson, R., Olsson, T. & Wigzell, H. (1998) *J. Exp. Med.* **187,** 1543–1548.
15. Matsumoto, Y., Jee, Y. & Sugisaki, M. (2000) *J. Immunol.* **164,** 2248–2254.
16. Matsumoto, Y. (2000) *J. Neuroimmunol.* **110,** 1–12.
17. Robinson, W. H., Fontoura, P., Lee, B. J., de Vegvar, H. E., Tom, J., Pedotti, R., DiGennaro, C. D., Mitchell, D. J., Fong, D., Ho, P. P., *et al.* (2003) *Nat. Biotechnol.* **21,** 1033–1039.
18. Garren, H., Ruiz, P. J., Watkins, T. A., Fontoura, P., Nguyen, L. T., Estline, E. R., Hirschberg, D. L. & Steinman, L. (2001) *Immunity* **15,** 15–22.
19. Fernandez-Vizarra, P., Fernandez, A. P., Castro-Blanco, S., Serrano, J., Bentura, M. L., Martinez-Murillo, R., Martinez, A. & Rodrigo, J. (2004) *Histol. Histopathol.* **19,** 823–844.
20. Oddo, S., Caccamo, A., Kitazawa, M., Tseng, B. P. & LaFerla, F. M. (2003) *Neurobiol. Aging* **24,** 1063–1070.
21. Oddo, S., Caccamo, A., Shepherd, J. D., Murphy, M. P., Golde, T. E., Kayed, R., Metherate, R., Mattson, M. P., Akbari, Y. & LaFerla, F. M. (2003) *Neuron* **39,** 409–421.
22. Oddo, S., Billings, L., Kesslak, J. P., Cribbs, D. H. & LaFerla, F. M. (2004) *Neuron* **43,** 321–332.
23. Monsonego, A., Zota, V., Karni, A., Krieger, J. I., Bar-Or, A., Bitan, G., Budson, A. E., Sperling, R., Selkoe, D. J. & Weiner, H. L. (2003) *J. Clin. Invest.* **112,** 415–422.
24. Qu, B., Rosenberg, R. N., Li, L., Boyer, P. J. & Johnston, S. A. (2004) *Arch. Neurol.* **61,** 1859–1864.
25. Monsonego, A., Maron, R., Zota, V., Selkoe, D. J. & Weiner, H. L. (2001) *Proc. Natl. Acad. Sci. USA* **98,** 10273–10278.
26. Yamamoto, S., Yamamoto, T., Kataoka, T., Kuramoto, E., Yano, O. & Tokunaga, T. (1992) *J. Immunol.* **148,** 4072–4076.
27. Krieg, A. M., Yi, A. K., Matson, S., Waldschmidt, T. J., Bishop, G. A., Teasdale, R., Koretzky, G. A. & Klinman, D. M. (1995) *Nature* **374,** 546–549.
28. Klinman, D. M., Yi, A. K., Beaucage, S. L., Conover, J. & Krieg, A. M. (1996) *Proc. Natl. Acad. Sci. USA* **93,** 2879–2883.
29. Gelman, A. E., Zhang, J., Choi, Y. & Turka, L. A. (2004) *J. Immunol.* **172,** 6065–6073.
30. Matsumo, Y., Sakuma, H., Miyakoshi, A., Tsukada, Y., Kohyama, K., Park, I. & Tanuma, N. (2005) *J. Neuroimmunol.* **170,** 49–61.
31. Beccaccio, G. L., Mor, F. & Steinman, L. (1999) *Int. Immunol.* **11,** 289–296.
32. Quintana, F. J., Rotem, A., Carmi, P. & Cohen, I. R. (2000) *J. Immunol.* **165,** 6148–6155.
33. Zhang, J., Wu, X., Qin, C., Qi, J., Ma, S., Zhang, H., Kong, Q., Chen, D., Ba, D. & He, W. (2003) *Neurobiol. Dis.* **14,** 365–379.
34. Hara, H., Monsonego, A., Yuasa, K., Adachi, K., Xiao, X., Takeda, S., Takahashi, K., Weiner, H. L. & Tabira, T. (2004) *J. Alzheimers Dis.* **6,** 483–488.
35. Sturchler-Pierrat, C., Abramowski, D., Duke, M., Wiederhold, K. H., Mistl, C., Rothacher, S., Ledermann, B., Burki, K., Frey, P., Paganetti, P. A., *et al.* (1997) *Proc. Natl. Acad. Sci. USA* **94,** 13287–13292.
36. Sturchler-Pierrat, C. & Staufenbiel, M. (2000) *Ann. N.Y. Acad. Sci.* **920,** 134–139.
37. Moechars, D., Lorent, K., de Strooper, B., Dewachter, I. & van Leuven, F. (1996) *EMBO J.* **15,** 1265–1274.
38. Calhoun, M. E., Wiederhold, K. H., Abramowski, D., Phinney, A. L., Probst, A., Sturchler-Pierrat, C., Staufenbiel, M., Sommer, B. & Jucker, M. (1998) *Nature* **395,** 755–756.
39. Danko, I., Fritz, J. D., Jiao, S., Hogan, K., Latendresse, J. S. & Wolff, J. A. (1994) *Gene Ther.* **1,** 114–121.
40. Sigurdsson, E. M., Scholtzova, H., Mehta, P. D., Frangione, B. & Wisniewski, T. (2001) *Am. J. Pathol.* **159,** 439–447.